

AN ABSTRACT OF THE THESIS OF

Grant Livingston for the Degree of Master of Science in Water Resources Engineering presented on June 8, 2015.

Title: Bioretention Establishment Hydrologic Characterization with Drift Correction and Calibration of Fine Water Level Measurements

Abstract approved:

Meghna Babbar-Sebens

ABSTRACT

Bioretention is a common form of green stormwater infrastructure that is used to attenuate peak flows from urban stormwater. Previous research shows that the bioretention peak response is not consistent across time or space and that the variables that affect peak hydrology are numerous. One variable that has not been well studied is bioretention establishment, or the indefinite period of time following installation during which the soils and plants mature until stabilization of hydrologic performance is achieved. Previous research has investigated changes in infiltration rate, but the peak flow response to this change in infiltration has not been quantified. The primary objective of this research was to characterize bioretention establishment peak hydrology. The runoff from a 9,300 m² drainage area was captured by a grey-green stormwater treatment train using an underground storage tank, a pump, and three parallel bioretention cells with underdrains. One of the cells was monitored for peak flows analysis from October 2014 to May 2015. The water level measurements were observed to drift by up to 29mm, introducing uncertainty into the flow rate measurements. A drift correction method was applied about every eight days to fix the drift. A water balance approach was then used to fine tune the outflow measurements for three storm events to minimize the residual of the water balance to less than 1% of the total inflow volume. Hydrologic function metrics of peak ratio and peak delay were then calculated to investigate the peak flow response to bioretention establishment. Mean peak ratios were 0.54, 0.68, and 0.61 and mean peak delays were 45 minutes, 63 minutes, and 59 minutes for the fall, winter and spring, respectively. No

significant differences between the peak ratios were found, however, at least one peak delay had a different mean than the other peak delays (1 way ANOVA, p value < 0.01). This indicates that the establishment period does indeed affect the peak flow hydrology. Future studies should attempt to minimize error in flow rate measurement to further characterize the establishment period and understand how it affects peak flows to improve bioretention design.

Keywords: Green stormwater infrastructure, bioretention, water quantity, pressure transducer bias correction, water balance, peak flow analysis, peak ratio, delay of peak, treatment train

©Copyright by Grant Livingston

June 8, 2015

All Rights Reserved

Bioretention Establishment Hydrologic Characterization with Drift Correction and
Calibration of Fine Water Level Measurements

by

Grant Livingston

A THESIS

Submitted to

Oregon State University

in partial fulfillment of

the requirements for the

degree of

Master of Science

Presented June 8th, 2015

Commencement June 2016

Master of Science thesis of Grant Livingston presented on June 8, 2015.

APPROVED:

Major Professor, representing Water Resources Engineering

Director of the Water Resources Graduate Program

Dean of the Graduate School

I understand that my thesis will become part of the permanent collection of Oregon State University libraries. My signature below authorizes release of my thesis to any reader upon request.

Grant Livingston, Author

ACKNOWLEDGEMENTS

I would like to thank my adviser, Dr. Meghna Babbar-Sebens, for her mentoring, valuable feedback, idea generation, and troubleshooting support. I would like to thank my committee member Dr. Arturo Leon for his assistance with facility design, hydraulic modeling, and valuable feedback. I would also like to thank my other committee members Dr. Yutaka Hagimoto and Dr. Tyler Radniecki for their valuable feedback and support. I would like to thank the funders of the research facility, including the Oregon Water Resources Department, Benton County Public Works, Oregon Built Environment and Sustainable Technologies (Oregon BEST), the Pacific Northwest Transportation Consortium (PacTRANS), and the City of Corvallis. I would especially like to thank Benton County and City of Corvallis staff, including Adam Stebbins and Iris Benson, for their support. I would like to thank David Eckert of the Corvallis Sustainability Coalitions Water Action Team, Maria Cahill of Green Girl Land Development Solutions LLC., and Dr. Desiree Tullos of Oregon State University for their input on the bioretention facility design. Finally, I would like to thank all of my lab mates, especially Chris Conatser, for their consistent assistance and support whenever I needed help with research problem solving.

TABLE OF CONTENTS

	<u>Page</u>
Introduction.....	1
Background	1
Previous Research	2
Methodology	6
Site Description	6
Design and Construction	7
Instrumentation and Monitoring	11
Pressure Transducer Drift Correction and Water Balance Calibration	12
Flowrate Calculations.....	14
Water Balance Calibration	15
Peak Hydrology Metrics.....	15
Bioretention Establishment Hydrologic Characterization.....	16
Results.....	17
Pressure Transducer Drift Correction	17
Cumulative Volumes	19
Fall, Winter, and Spring Storm Water Balance Calibration	20
Peak Flow Response to Establishment Measured by Hydrologic Metrics.....	25
Drain Tests	29
Discussion	31

Pressure Transducer Drift Correction	31
Water Balance Calibration	32
Bioretention Establishment	33
Peak Flow Analysis.....	33
Error Analysis	38
Flowrate Calculations	38
Additional Sources of Pressure Transducer Measurement and Flow Calculation Error	40
Conclusions	43
Considerations for Future Research in Bioretention.....	44
Bibliography	46
Appendix A: Plant List	49

LIST OF FIGURES

<u>Figure</u>	<u>Page</u>
Figure 1: Conceptual diagram of bioretention establishment.	4
Figure 2. Schematic of the bioretention facility.....	8
Figure 3. Typical bioretention cross section with meander, soil media, construction sand, crushed gravel, round river rock, underdrain, and impermeable liner.	9
Figure 4. Bioretention facility plan view. Note that dotted and dashed lines are perforated and solid pipes, respectively, below ground level.	10
Figure 5. The change of water level height from during a storm to after a storm. The relationship between h_{measured} and h_{weir} after a storm event is the basis for the drift correction.	13
Figure 6. The observed sediment bay 1.5m range SDX pressure transducer drift (top) and drift corrected data (bottom). The physically measured distance for h_{weir} (255mm) was subtracted from h_{measured} to obtain h_v (top). The relatively stable h_{weir} intervals, highlighted in green, were applied to their applicable ranges (generally 1 storm) to complete the drift correction. The high frequency of peaks is due to the automatic pump turning on and off in response to precipitation.	18

Figure 7. The total cumulative inflows were greater than the total cumulative outflows by 370 m³, and they could not be accounted for by the change in soil water storage alone. The data gap between late January and late February was due to sensor failure..... 19

Figure 8. Drift corrected, pre-water balance calibrated flows. Storm events from fall 2014, winter 2014-2015, and spring 2015. 23

Figure 9. The drift corrected and water balance calibrated flow data were characteristic of the expected flow response: the water level drains to the bottom of the V before becoming relatively stable, and the outflow continues between peak flows due to gradual drainage of soil water. 24

Figure 10. The peak finder was parameterized using the three storm events, and then it was used to find the peaks from the remainder of the drift corrected dataset. 26

Figure 11. Histogram of peak ratio for each season. The distributions have a similar range of variance, which validates the assumption of similar spreads for the 1 way ANOVA..... 27

Figure 12. Histogram of peak delay for each season. The distributions have a similar range of variance, which validates the assumption of similar spreads for the 1 way ANOVA..... 28

Figure 13. Results from the drain tests are characterized by sharps peaks followed by gradual recession curves. The recession curve in Test #2 had a more gradual slope than Test #1. 30

Figure 14. Photos of plant growth throughout the monitoring period.	37
Figure 15. Variation of error with water depth for the inflow rate measurements. The error decreases exponentially as the head behind the V-notch weir increases.	39
Figure 16. The range of error for the inflow and outflow measurements based on a 3.8mm accuracy of the 1.5m SDX pressure transducers. The three lines for the inflow and outflow rates are the minimum, mean, and maximum estimated flowrates based on the manufacturer's specified water level measurement error.	40

LIST OF TABLES

<u>Table</u>	<u>Page</u>
Table 1. Review of bioretention peak hydrology literature. n Storms = # storms analyzed, A_{BR} = bioretention area. A_{CT} = catchment area, R_{peak} = peak ratio. P_{delay} = peak delay, reported as typical or mean value. *lag time was reported instead of peak delay. **Average of 180 min for medium rain, and 80 min for heavy rain.	3
Table 2. The volume of each element in the water balance was calculated. The $V_{underdrain}$ and residual are highlighted for comparison with Table 3.*The error is reported as the residual's percentage of the total inflow volume.	20
Table 3. The pumped inflow volume and underdrain outflow volume changed for each storm from the pre-calibration volume balance to the post-calibration volume balance due to the h_{weir} adjustments. *The error is reported as the residual's percentage of the total inflow volume.....	21
Table 4. Outflow h_{weir} calibration was accomplished by minimizing the difference between the target (the drift corrected water balance residual) and the estimated underdrain outflow volume, $V_{underdrain}$, through iteration.	21
Table 5. Peak ratio and peak delay statistics. The low P-value for the one-way ANOVA test on differences between means for the peak delay was statistically significant.	29

INTRODUCTION

Background

Urbanized landscapes increase hydrologic peak flowrates and decrease hydrologic peak delays resulting in flashier hydrographs compared to pre-development hydrologic regimes (Leopold 1975); (EPA 1993). Flashy hydrographs are characterized rapidly occurring, large magnitude waterway peaks following the onset of precipitation. The reason this occurs is that conventional stormwater infrastructure, such as gutters, ditches, and pipes, along with impervious surfaces, such as roofs, parking lots, and roads, increases the rate of stormwater conveyance. By concentrating a catchment area's runoff into a relatively small impermeable drainage system, there is an increased potential for downstream flooding compared to the pre-development landscape (Meierdiercks 2010); (Fletcher et al. 2013). For example, a 10-year storm in a developed area can produce the runoff equivalent of a 25-year storm (Hollis 1975). Wastewater treatment facilities are frequently overwhelmed by the excessive volumes of stormwater and use combined sewer overflows as a method to manage the urban influent. These combined sewer overflows spill raw sewage into urban waterways. Furthermore, urban stormwater runoff causes an overall degradation of urban stream ecosystems in a condition known as "urban stream syndrome" (Walsh et al. 2005) due to both hydrologic impacts as well as water quality impacts.

Low impact development, (LID), also known as green stormwater infrastructure (GSI) in the Pacific Northwest, was first introduced the early 1990s in Prince George's County, Maryland (Roy-Poirier et al. 2010). LID aims to control the stormwater runoff from a developed site so that the hydrology and water quality approximate that of the pre-development site hydrologic conditions (Davis 2008). LID has gained considerable interest in recent years for addressing the

water quantity and water quality issues associated with urban runoff (EPA 2013). Several major cities in the United States have already started implementing GSI on a large scale, including Philadelphia, Seattle, and Portland (Garrison et al. 2013). One of the most well studied forms of GSI is bioretention.

Bioretention has the potential to address the issues associated with conventional stormwater infrastructure. Bioretention has been defined as “a landscaped depression that receives runoff from up gradient impervious surfaces, and consists of several layers of filter media, vegetation, an overflow weir, and an optional underdrain,” (Liu et al. 2014). Bioretention is used to reduce the effects of hydromodification (Poresky and Palhegyi 2008), stormwater pollution (EPA 1999), and combined sewer overflows (Clayden and Dunnett 2007); (Cramer 2012). Some examples of bioretention include rain gardens, bioswales, and stormwater planters.

Previous Research

Field studies have shown that bioretention practices reduce impervious surface hydrologic impacts by reducing peak magnitudes and delaying the time to the peak (Table 1). The hydrologic function of a bioretention facility can be described with the metrics of peak ratio and peak delay. The peak ratio is the ratio of peak outflow to peak inflow, and the peak delay is the elapsed time between inflow and outflow peaks. A complete description of these metrics can be found in the methods. The variables that can affect hydrologic function include regional hydrology, drainage configuration, and surface storage volume (Brown et al. 2013). Additional variables include media depth (Brown and Hunt 2010), media composition (Carpenter and Hallam 2009); (Hsieh and Davis 2005); (Paus et al. 2014), antecedent moisture conditions (Davis 2008); (Muthanna et al. 2008),

plant selection; (Le Coustumer et al. 2012) ; (Barrett et al. 2012) , and season (Hunt et al. 2008); (Emerson and Traver 2008).

Author	Year	Location	n Storms	A _{CT}	A _{BR}	A _{BR} /A _{CT}	R _{Peak}			P _{delay}
				m ²	m ²		Median	Mean	Std. Dev.	minutes
Davis	2008	Maryland	49	1260	28	2.2%	0.51	0.48		120
		Maryland	49	1260	28	2.2%	0.42	0.40		
Dietz and Clausen	2005	Connecticut	1	107	9	8.6%		0.35		60
Hatt et al.	2009	Melborne, Australia	17	4500	15	0.3%	0.18	0.21	0.13	
		Melborne, Australia	4	1000	20	2.0%	0.15	0.16	0.03	
Hunt et al.	2008	North Carolina	16	3700	229	6.2%	0.01	0.01	0.01	180
Li et al.	2009	Maryland	22	2600	181	7.0%	0.14			
		Maryland	60	4500	102	2.3%	0.02			
		North Carolina	46	5000	317	6.3%	0.01			
		North Carolina	46	4800	317	6.6%	0.01			
		North Carolina	31	3600	162	4.5%	0.04			
		North Carolina	33	2200	99	4.5%	0.1			
Muthanna et al.	2008	Norway	44	20	1	4.8%	0.65	0.56	0.29	90*
Olszewski and Davis	2013	Maryland	197	3700	102	2.8%		0.83		
Passeport	2009	North Carolina	16	3450	102	3.0%		0.82		
		North Carolina	13	3450	102	3.0%		0.86		
Schlea et al.	2014	Ohio	4	2894	27	0.9%	0.46	0.42	0.32	16
		Ohio	3	869	19	2.1%	0.29	0.31	0.28	
UNHSC	2012	New Hampshire				12.5%		0.25		266*
		New Hampshire				0.6%		0.21		309*
		New Hampshire				0.6%		0.16		216*
		New Hampshire				3.1%		0.5		61*
Yang et al.	2013	Ohio State University	8	63	14	22.1%		0.17		130**

Table 1. Review of bioretention peak hydrology literature. n Storms = # storms analyzed, A_{BR} = bioretention area. A_{CT} = catchment area, R_{peak} = peak ratio. P_{delay} = peak delay, reported as typical or mean value. *lag time was reported instead of peak delay. **Average of 180 min for medium rain, and 80 min for heavy rain.

The range of values reported for peak ratio and peak delay in **Table 1**, along with the variables stated above, complicate the process of accurately upscaling bioretention models from the site scale to watershed scale. Additionally, unlike conventional stormwater infrastructure, bioretention facilities are dynamic living systems which grow and change over time. At present, there is still a lack of a model that can be used at the design stage to accurately predict bioretention hydrologic function (Liu et al. 2014). Models may not be able to be upscaled at this time because of the numerous variables affecting flows that can vary from one site to another that are not well represented with a single parameter. This is an issue because urban planners need to design functional stormwater systems at large scales, but engineers and landscape architects still do not

have the tools necessary to be able to accurately estimate hydrologic function of bioretention systems at the site scale to meet specific criteria for urban stormwater management. By improving the understanding of the variables that affect hydrologic function, such as peak ratio and peak delay, bioretention modelers can improve the process of upscaling bioretention design from site scale to watershed scale, and therefore help to mitigate the negative impacts associated with urban hydrology.

One of the variables that affects bioretention hydrology that has not been well studied is bioretention establishment, which is defined here as the indefinite period of time following bioretention construction and planting activities until the system shows stability in hydrologic function. Previous work in bioretention establishment has investigated soil permeability's response to preferential flow path development. A trend of decreased permeability followed by increased permeability has been attributed to surface clogging and soil media compaction followed by macropore and preferential flow path development (Hatt et al. 2009), see **Figure 1**.

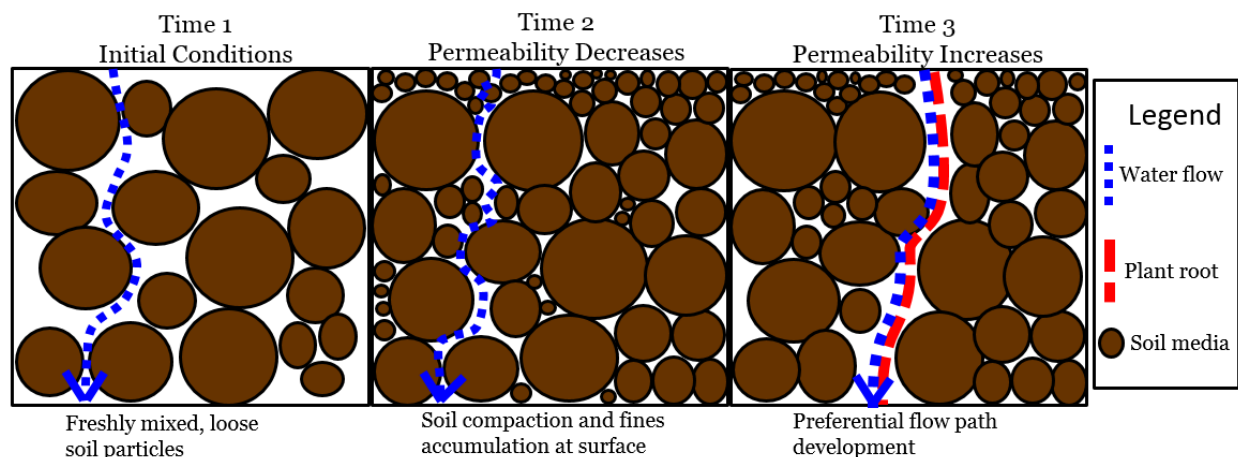


Figure 1: Conceptual diagram of bioretention establishment.

Both vegetation (Le Coustumer et al. 2012) and earthworms through bio-perturbation (Greene et al. 2009) have been shown to maintain or increase soil permeability over time. However, the effect

of bioretention establishment on peak flow hydrology has not been well researched. A greater understanding of bioretention establishment could help stormwater managers to properly design bioretention systems to meet stormwater management criteria. For example, if the establishment is an important variable in affecting the hydrologic function, perhaps it could be controlled through the use of specific a soil media, vegetation selection, and underdrain configuration to meet stormwater management objectives.

In this field scale study, a newly constructed bioretention cell was monitored from October 21st 2014 to May 15th 2015 in Corvallis, Oregon. The primary objective of this research was to characterize bioretention establishment from a hydrologic perspective. The main question that was investigated is *how does bioretention hydrologic function change from initial conditions in the fall to an unknown establishment state in the spring?* This question was answered using inflow and outflow rates, which were verified with a drift correction method of water level measurement and a water balance calibration (LeFevre et al. 2009). The results can be used by bioretention designers to gain a greater understanding of the peak flow variability caused by bioretention establishment, and the methods can be used to improve future bioretention monitoring studies.

METHODOLOGY

Site Description

The *OSU-Benton County Green Stormwater Infrastructure Research Facility, and Oregon Best Lab* is a three cell bioretention facility, installed in the summer of 2014, which captures runoff from the Benton County Public Works transportation yard. This 9,300 m² catchment area is used to store equipment and materials for road construction. It consists of large trucks and tractors, road fill and base material, raw asphalt, paint, a refueling station, and a staff parking lot. LiDAR point cloud data of the site was used to estimate the catchment boundary, and it was confirmed with field evaluation during a runoff producing storm event.

About 59% of the catchment area is impermeable with asphalt or a roof, and the other 41% is clay with gravel on top that has been highly compacted from all of the heavy equipment. This clay section is also relatively impermeable. The average annual precipitation is 1,100 mm with most of the precipitation falling during the fall, winter, and spring. The native plant selection was guided by a local Willamette River historian who confirmed that the area surrounding the catchment was Willamette Valley wetland prairie and prairie habitat prior to Euro-American settlement (Benner 2015), which

Before project implementation, the runoff from the catchment area flowed into the City of Corvallis' piped stormwater network and into the local Mill Race Creek. This creek currently is managed to drain stormwater from southern Corvallis into the Marys River. In a preliminary fish survey conducted by the Oregon Department of Fish and Wildlife, the Mill Race found to host

spring Chinook salmon, a federally listed endangered species (Hans 2015), which is important for stormwater management decisions.

Design and Construction

The design of the bioretention cells was guided by the Oregon State University Stormwater Extension rain garden sizing spreadsheets and drawing design details (Extension 2014), the LID Center bioinfiltration sizing spreadsheets (Low Impact Center Development 2015), and the Oregon Rain Garden Guide (Emanuel et al. 2009). Runoff from the catchment area is intercepted by an inline 6,700 L concrete underground storage tank, and pumped at approximately 2.2 L/s by a Liberty 251 automatic pump into a 5,500 L concrete sedimentation bay. Water then flows by gravity through the weirs and into the bioretention cells for treatment. After flowing through the

soil, sand, and gravel media layers, the water flows into a 15 cm (6 in.) perforated underdrain that connects to the existing stormwater pipe network. See **Figure 2** for a schematic of the facility.

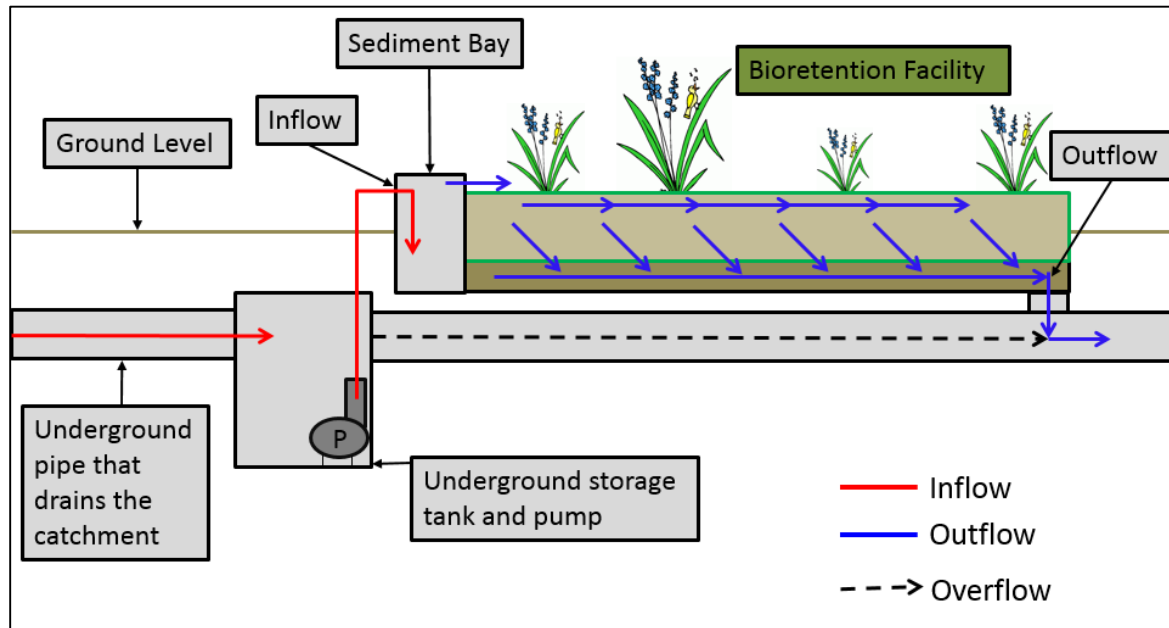


Figure 2. Schematic of the bioretention facility.

Three 90° V-notch weirs were installed at the same level in the sediment bay to allow for equal stormwater flow into each of the 3.2 m wide by 28.5 m long parallel bioretention cells. The weirs were sized by modeling the pump and dividing its flow into three weirs and by using a standard weir equation to model the flow of water through the weirs. Vertical walls made from steel H-piles and repurposed lumber separated the cells, and a 1.1 mm (45 mil) EPDM fish safe pond liner was installed around the walls and in the cells to prevent flow interference between cells and with the groundwater table. See Figure 3 for a typical cross section and Figure 4 for a plan view of the site.

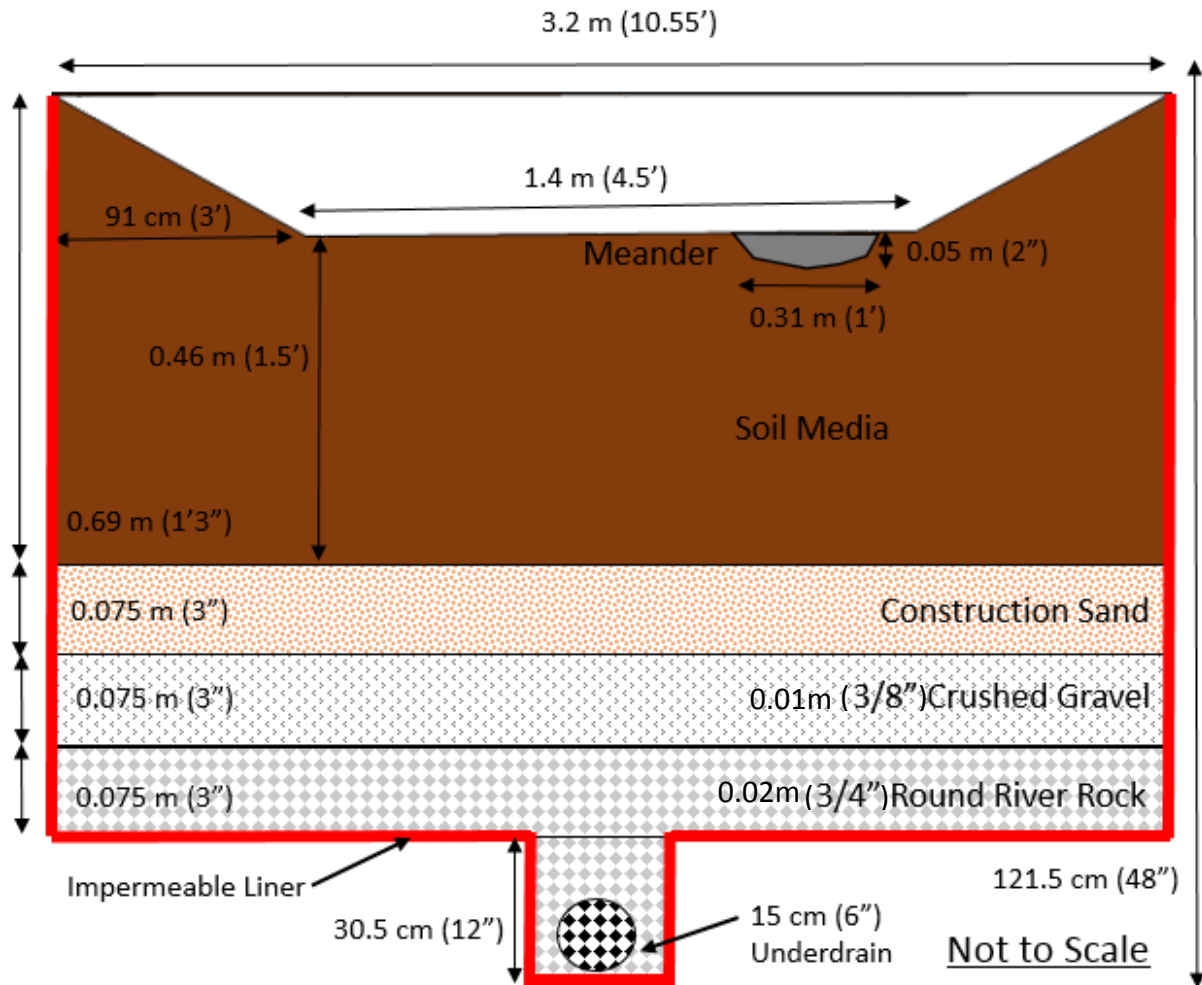


Figure 3. Typical bioretention cross section with meander, soil media, construction sand, crushed gravel, round river rock, underdrain, and impermeable liner.

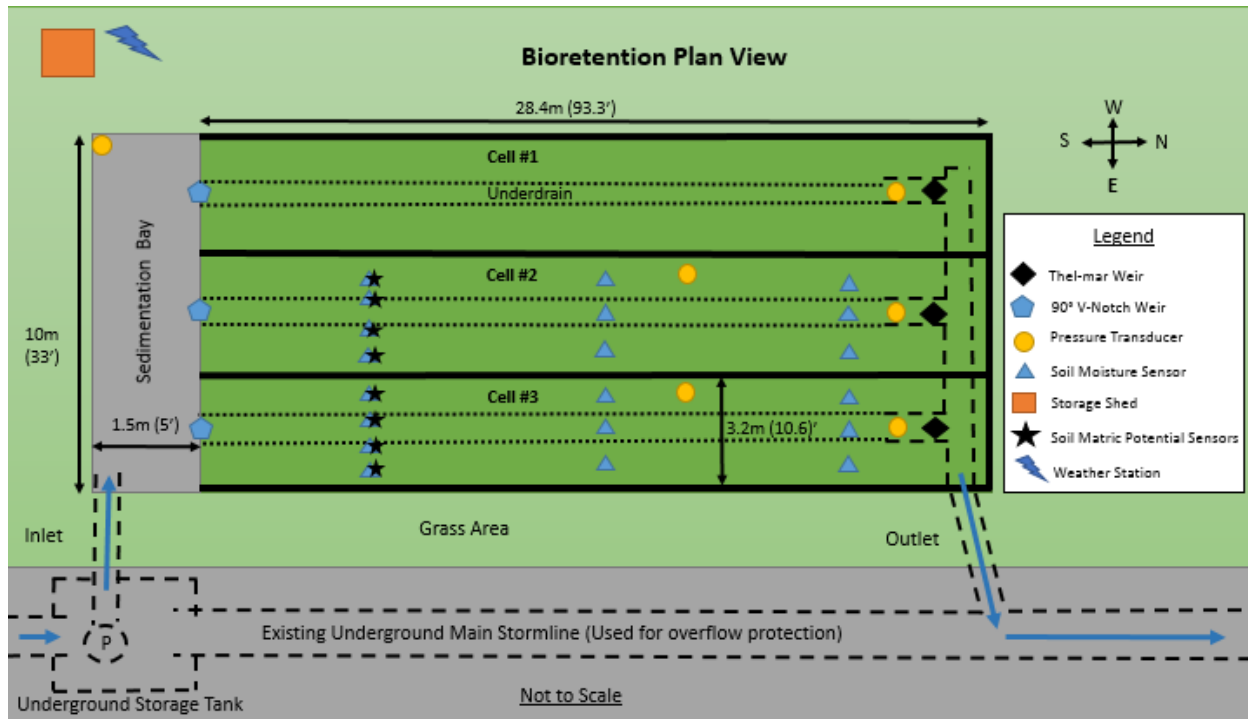


Figure 4. Bioretention facility plan view. Note that dotted and dashed lines are perforated and solid pipes, respectively, below ground level.

A 152 mm (6 in.) thin wall perforated underdrain pipe was placed at the bottom of each cell above the impermeable liner and covered with a non-woven 170g (6 oz) geotextile to prevent clogging. The storage/filtration layers in the facility consist of 1.9 cm (3/4 in.) rounded river rock, 0.95 cm (3/8 in.) crushed gravel, and construction sand. The soil media consisted of a 2:1:1 mixture of the site's native silty clay loam, municipal yard waste compost (as a source of nutrients for the plants), and mint compost (as a source of organic matter). The swale side slopes were 4:1. A 1.9cm (3/4 in.) rounded river rock meander underlain by landscape fabric was installed in the center of the swales for aesthetics and increased flow conveyance. A drip irrigation system was installed to keep the plants alive during the dry summers which are typical of the Willamette Valley region.

Cell 1 was left as bare soil, Cell 2 was planted with native grasses, and Cell 3 was planted with mixed vegetation. The dataset from Cell 3 was the most complete, therefore it was used in the

following analysis. The Cell 1 dataset lacked fall and spring data, and the Cell 2 dataset lacked winter data. Planting activities primarily took place in mid-September, however, additional seeds and bulbs were added throughout the fall, and several native plants came in on their own, possibly from the native soil's seed bank. See Appendix A for a full list of plant species used in Cell 3. The bioretention cells were maintained with manual hand weeding in the beginning of spring.

Instrumentation and Monitoring

The influent water level height used for flow rate calculations was monitored with a pressure transducer anchored onto the concrete wall of the sediment bay. Initially, a Steven's SDX 1.5m (5 ft) range pressure transducer was installed, however, it failed on January 23, 2015, and water level data was not collected again until a temporary replacement Decagon CTD-10 was installed on February 26, 2015. A more accurate 0.76m (2.5ft) range SDX pressure transducer replaced the Decagon CTD-10 on April 9, 2015 until the end of the monitoring period on May 15th, 2015.

The underdrain effluent was monitored with a SDX 1.5m (5 ft) range pressure transducers installed in a stilling well upstream of a 15.2cm (6 in.) Thel-Mar compound weir. Overflows were not monitored, but were assumed to be negligible based on field observations during heavy storm events. A MetONE Weather Station was used to measure wind speed, wind direction, relative humidity, air temperature, and barometric pressure. An Apogee SP-212 pyranometer was used to measure solar radiation, and a MetONE tipping bucket rain gauge was used to monitor precipitation. Soil moisture and temperature was measured with 10 Steven's Hydraprobe II sensors, and soil matric potential was measured with TensioMark Tensiometers. All of the data was logged at 15 minutes intervals with a Campbell Scientific CR 1000 Data Logger powered by

a 100W solar panel and 12V lead-acid deep cycle battery. The relative placement of the instrumentation can be viewed in **Figure 4** above. Note that only the data from Cell 3 was used in this study.

Pressure Transducer Drift Correction and Water Balance Calibration

The datum for the inlet and outlet pressure transducers drifted over time, which is common for fine scale water level sensors (Sorensen and Butcher 2011) and has been corrected in previous literature (LeFevre et al. 2009). The correction of the drift was made possible due to the physical setup of the weirs. After a storm event, the water level would drain to the bottom of the weirs and stabilize until the next storm event or evapotranspiration occurred. The data was adjusted by locating intervals of time where the data showed that the water level was stable at the bottom of the weir following a storm event. The distance between the pressure transducer's zero water line and the bottom of the V-notch weir is referred to as h_{weir} for the remainder of this report. Notice that h_{measured} , the pressure transducer's measured water level, is equal to h_{weir} after a storm event. This physical process that lead to the relationship between h_{measured} and h_{weir} was used as the basis for the drift correction method. See **Figure 5** for reference.

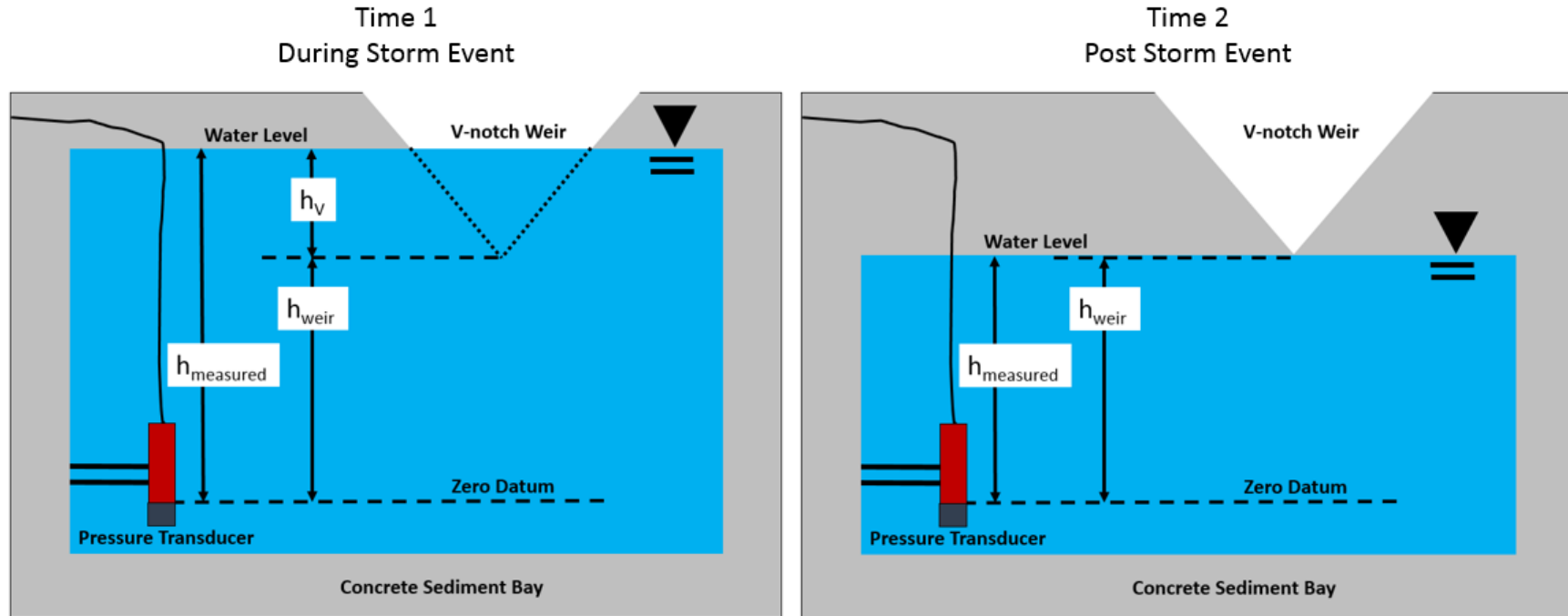


Figure 5. The change of water level height from during a storm to after a storm. The relationship between h_{measured} and h_{weir} after a storm event is the basis for the drift correction.

The general procedure for the drift correction was as follows:

1. Find a relative stable interval of h_{measured} equal to h_{weir} following a storm event using graphical analysis and examination of the water level time series numerical data.
2. Find the average value of h_{weir} for the stable interval.
3. Find the applicable range of each h_{weir} in the water level time series dataset, and subtract h_{weir} from h_{measured} to obtain h_v for flowrate calculations (see Volumetric Water Balance below).

The applicable range of h_{weir} was determined through graphical analysis by using a horizontal line placed at the average value of h_{weir} and observing where the line no longer matched with the relatively stable measured water level following a storm event.

Flowrate Calculations

Flowrates were calculated using the drift corrected values of h_v . An additional 2mm was added to h_v to account for the curvature at the bottom of the V-notch weir, which kept water from draining down to the exact vertex of the V. The inflow rates, Q_{in} (m^3/s), were calculated with a standard V-notch weir equation (Eqn. 1).

$$Q_{\text{in}} = \frac{8}{15} C_d (2g)^{\frac{1}{2}} \tan\left(\frac{\theta}{2}\right) h_v^{5/2} \quad \text{Eqn. 1}$$

Where g (m/s^2) is gravity, and θ (radians) is the angle of the v-notch. A standard value of 0.6 was used for the coefficient of discharge, C_d (unitless).

The outflow rates were calculated using a rating curve that was based on linear interpolation of the discharge table provided by the weir manufacturer, Thel-Mar. All outflow rate calculations used the drift corrected dataset except for the three storm events discussed below, which used both the drift corrected and water balance calibrated dataset.

Water Balance Calibration

A novel method using a water balance approach was used to calibrate the h_{measured} value for the underdrain stilling well pressure transducer. The water balance was computed for three 96 hour storm events (fall, winter, spring) using system inputs of cumulative weir inflow, V_{pumped} , and cumulative direct precipitation on the facility, V_{precip} . System outputs included cumulative underdrain weir outflow, $V_{\text{underdrain}}$, and cumulative evapotranspiration, V_{ET} (Eqn. 2).

$$V_{\text{pumped}} + V_{\text{precip}} - V_{\text{underdrain}} - V_{\text{ET}} = \Delta S \quad \text{Eqn. 2}$$

The change in storage, ΔS , was computed using the average change of the 10 soil moisture sensors in the bioretention cell before and after the storm events, which was multiplied by the volume of the soil media using an average depth of 0.6m. The reference evapotranspiration, V_{ET} , was calculated with daily maximum and minimum temperatures using the Hargreaves method (Allen et al. 1998) with the Samani correction (Samani 2000).

The total volume, V , of each 96 hour storm event was computed using a trapezoidal numerical integration of the volume flux, Q , with a time step, Δt , of 15 minutes (Eqn. 3).

$$V = \int_{t_1}^{t_n} Q \, dt = \sum_{i=1}^{i=n} ((Q_{t_i} + Q_{t_{i+1}})/2 * \Delta t) \quad \text{Eqn. 3}$$

The residual of the water balance was used to calibrate the underdrain stilling well's value for h_v by minimizing the difference between the residual and the total outflow volume.

Peak Hydrology Metrics

Bioretention hydrologic performance was quantified with the metrics of peak flow ratio (Davis 2008) and the peak delay time. See Eqns. 4-5.

$$R_{\text{peak}} = \frac{Q_{\text{peak-out}}}{Q_{\text{peak-in}}} \quad \text{Eqn. 4}$$

Where $Q_{\text{peak-in}}$ (L/s) is the peak inflow rate, and $Q_{\text{peak-out}}$ (L/s) is the corresponding peak outflow rate.

$$P_{\text{delay}} = T_{Q_{\text{peak-out}}} - T_{Q_{\text{peak-in}}} \quad \text{Eqn. 5}$$

Where P_{delay} is the difference in the elapsed time between the inflow peak ($T_{Q_{\text{peak-in}}}$) and its paired outflow peak ($T_{Q_{\text{peak-out}}}$). In general, a lower value of R_{peak} is desirable because it means that the outflow peak is smaller in magnitude than the inflow peak, and a higher value of P_{delay} is desirable because it means that the outflow peak was delayed by greater period of time.

Bioretention Establishment Hydrologic Characterization

Bioretention establishment was characterized with a peak flow hydrologic function analysis and with two drain tests. The peak flow monitoring period took place during the fall, winter, and spring of 2014-2015. Peak ratio and peak delay statistics were computed for each season and compared to investigate the peak hydrologic response of bioretention establishment. The drain tests were conducted under saturated conditions in November 2014 (fall) and March 2015 (spring) by closing the underdrain outlet valves and allowing the cells to pond and reach overflow conditions. Once saturated and ponded, the underdrain outlet valves were opened, and the cells were drained while measuring the change in water level behind the underdrain outflow weir. Water level height for the outflow recession curve was collected and compared for these two drain tests to characterize the effect of establishment on soil water flow.

RESULTS

Pressure Transducer Drift Correction

Pressure transducer water level measurement drift was observed throughout the monitoring period. The drift in the sediment bay pressure transducers had a magnitude of 29mm for the 1.5m range Steven's SDX pressure transducer over the course of 93 days, 18 mm for the Decagon CTD pressure transducer (42 days), and 2mm for the Steven's 0.76m pressure transducer (36 days). The underdrain stilling well pressure transducer had a drift of 25mm over the course of the 274 day during the monitoring period.

A total of 21 drift corrections were made for the sediment bay pressure transducers and 22 for the underdrain stilling well pressure transducer. A drift correction was applied on average every 8.1 days with a standard deviation of 8.4 days for the sediment bay pressure transducers, and 7.8 days with a standard deviation of 4.8 days for the underdrain stilling well pressure transducers.

An example of the drift correction can be seen in **Figure 6**.

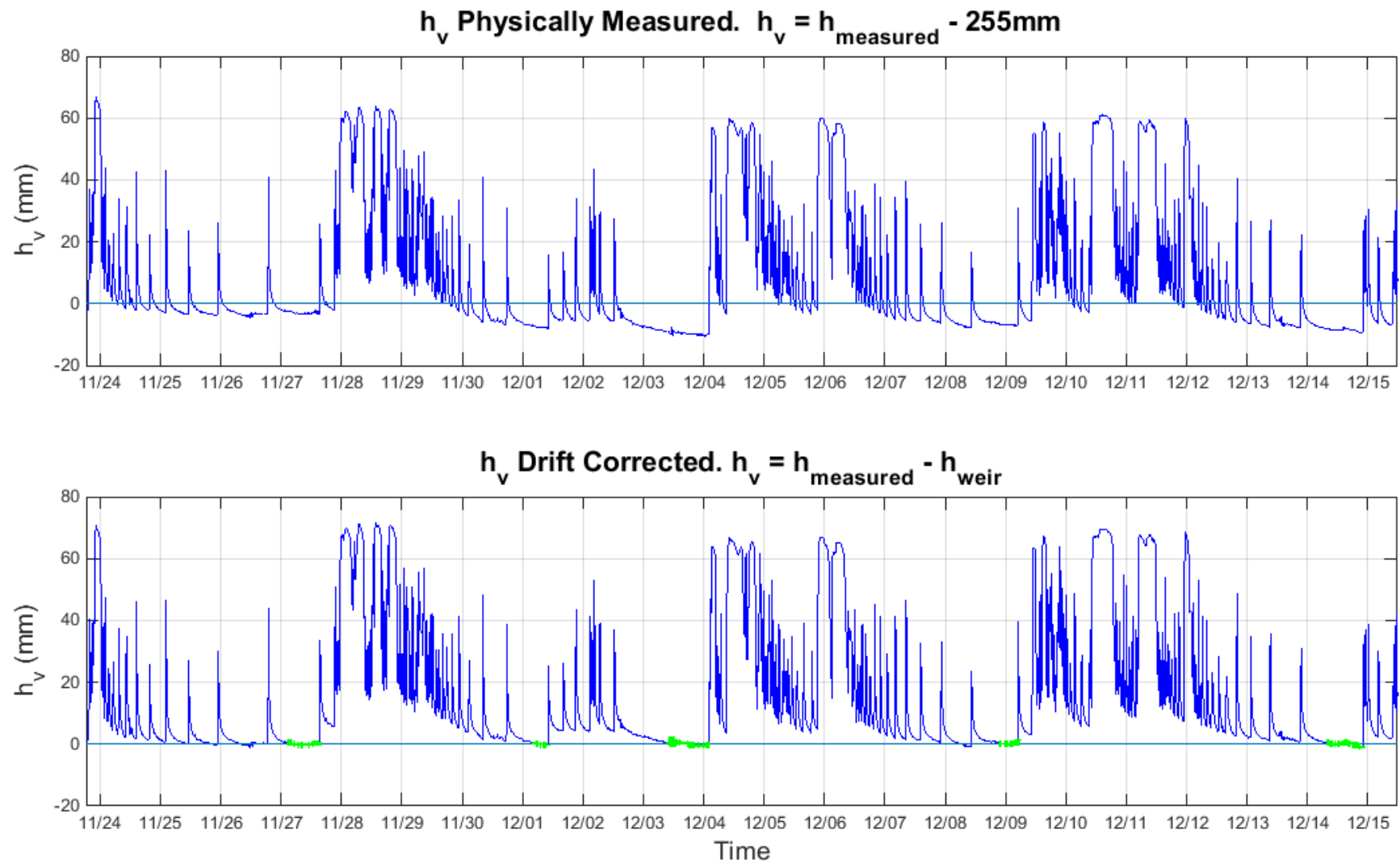


Figure 6. The observed sediment bay 1.5m range SDX pressure transducer drift (top) and drift corrected data (bottom). The physically measured distance for h_{weir} (255mm) was subtracted from h_{measured} to obtain h_v (top). The relatively stable h_{weir} intervals, highlighted in green, were applied to their applicable ranges (generally 1 storm) to complete the drift correction. The high frequency of peaks is due to the automatic pump turning on and off in response to precipitation.

Water Balance

Cumulative Volumes

The drift corrected data were used to calculate cumulative inflow and outflow volumes for the water balance verification. Cumulative inflow and outflow volumes were calculated from the flow rates using a trapezoidal method for numerical integration. The cumulative volumes were compared to visualize the water balance, see **Figure 7**.

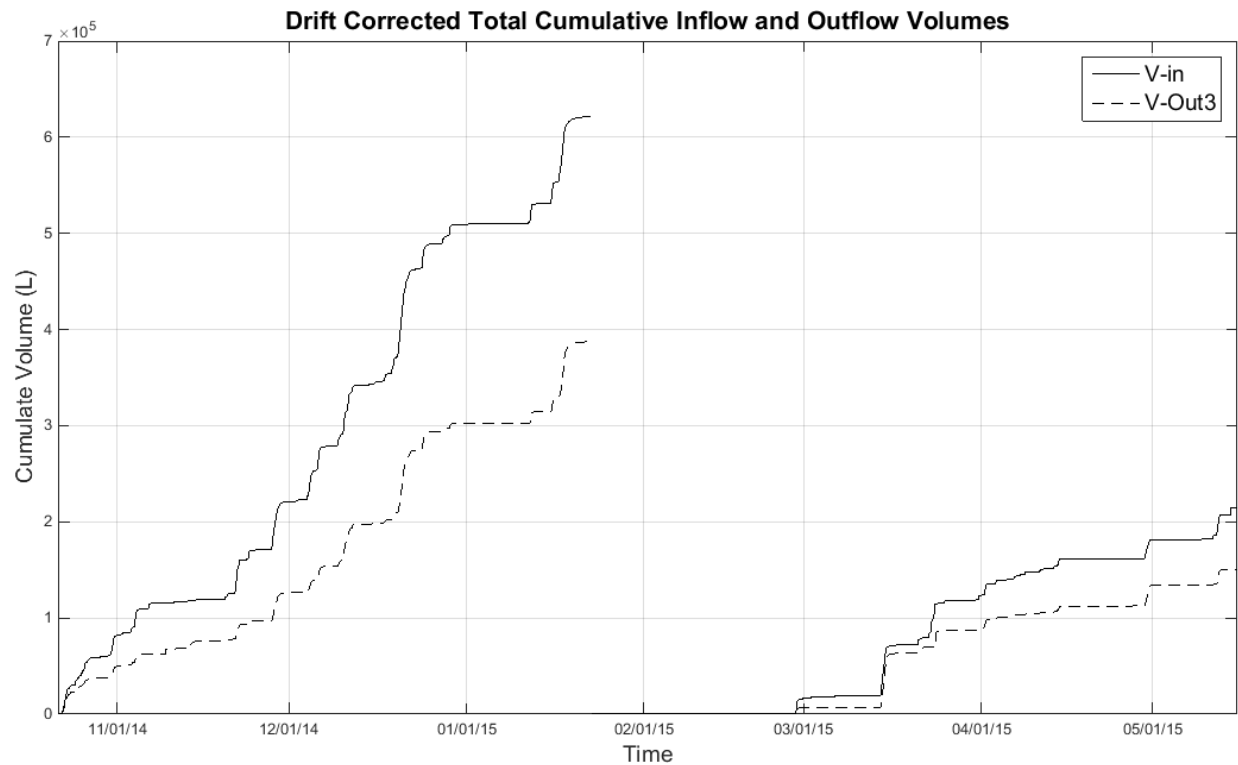


Figure 7. The total cumulative inflows were greater than the total cumulative outflows by 370 m³, and they could not be accounted for by the change in soil water storage alone. The data gap between late January and late February was due to sensor failure.

The shape of the inflow and outflow curves are in sync, but the inflow curve grows more rapidly.

The total inflow volume was 900 m³, the total outflow volume was 530 m³, and the total estimated pore space was 26 m³ (assuming a soil porosity of 0.5). The difference between the total inflows (weir inflow and direction precipitation) and outflows (underdrain outflow and evapotranspiration)

could not be accounted for by the change in the soil water storage alone. Therefore, the water balance was not validated. Likely sources of error include the weir inflow and outflow estimations which were based on the water level height measurements used in the flowrate calculations, as well as the drift correction procedure. A water balance approach, described below, was used to calibrate the flow rate data.

Fall, Winter, and Spring Storm Water Balance Calibration

Three storm events were selected from the fall, winter, and spring for water balance analysis.

The h_{weir} values from the underdrain stilling well pressure transducer were calibrated to “close” the water balance. Estimated evapotranspiration and direct precipitation values were kept constant, as they were 1 to 3 orders of magnitude smaller than the weir flow values and considered negligible. Target values for each outflow h_{weir} calibration were calculated as the residual of the volumetric water balance for each storm event. Residuals were on the same order of magnitude as the total inflow volume before the water balance calibration, and were decreased to less than 1% of the total inflow volume after the water balance calibration. The percent error, calculated as the residuals’ percentage of the total inflow volume, decreased from 61%, 66%, and 47% to 0.85%, 0.09%, and 0.17% for the fall, winter, and spring storms respectively (**Table 2**) and (**Table 3**).

Pre-Calibration Volume Balance							
Storm	V_{pumped}	V_{precip}	$V_{\text{underdrain}}$	V_{ET}	ΔS	Residual	Error*
Season	L	L	L	L	L	L	%
Fall	3.2E+04	2.0E+03	1.5E+04	8.3E+01	-1.4E+03	2.1E+04	61%
Winter	2.2E+04	1.1E+03	8.3E+03	3.8E+01	-3.8E+02	1.5E+04	66%
Spring	1.9E+04	2.5E+03	1.1E+04	1.4E+02	3.8E+02	1.0E+04	47%

Table 2. The volume of each element in the water balance was calculated. The $V_{\text{underdrain}}$ and residual are highlighted for comparison with Table 3.*The error is reported as the residual’s percentage of the total inflow volume.

Post-Calibration Volume Balance							
Storm	V _{pumped}	V _{precip}	V _{underdrain}	V _{ET}	ΔS	Residual	Error*
Season	L	L	L	L	L	L	%
Fall	3.2E+04	2.0E+03	3.6E+04	8.3E+01	-1.4E+03	288	0.85%
Winter	2.2E+04	1.1E+03	2.4E+04	3.8E+01	-3.8E+02	20	0.09%
Spring	1.9E+04	2.5E+03	2.1E+04	1.4E+02	3.8E+02	38	0.17%

Table 3. The pumped inflow volume and underdrain outflow volume changed for each storm from the pre-calibration volume balance to the post-calibration volume balance due to the h_{weir} adjustments. *The error is reported as the residual's percentage of the total inflow volume.

The h_{weir} values were adjusted to the nearest 0.1mm to minimize the difference between the underdrain outflow volume and the target volume. The h_{weir} values were decreased by 7.0mm, 7.8mm, and 5.7mm for the fall, winter, and spring, storms respectively, which causes the apparent outflow rates to increase. See **Table 4** for an example of the iterations used to calibrate h_{weir} .

Outflow h_{weir} Calibration by Volume Balance									
Trial	Fall Storm			Winter Storm			Spring Storm		
	h_{weir} adjustment	V _{underdrain}	Difference	h_{weir} adjustment	V _{underdrain}	Difference	h_{weir} adjustment	V _{underdrain}	Difference
	mm	L	L	mm	L	Balance	mm	L	Balance
1	5	28,150	7,204	5	16,525	7,115	5	19,554	1,649
2	6	31,784	3,570	7	21,334	2,306	5.5	20,689	515
3	6.9	34,847	507	7.7	23,325	315	5.6	20,926	277
4	7	35,642	(288)	7.8	23,620	20	5.7	21,165	38
5	7.1	36,043	(689)	7.9	23,922	(282)	5.8	21,407	(203)
6	8	39,816	(4,462)	8	24,228	(588)	8	27,284	(6,081)
	Target:	35,354	L	Target	23,640	L	Target	21,203	L

Table 4. Outflow h_{weir} calibration was accomplished by minimizing the difference between the target (the drift corrected water balance residual) and the estimated underdrain outflow volume, V_{underdrain}, through iteration.

Once the underdrain stilling well h_{weir} values were calibrated to decrease the water balance residuals to below 1% of the total inflow, the h_{weir} values were subtracted from the h_{measured} values to obtain calibrated h_v for flowrate calculations. These flowrates calculations for the fall, winter, and spring storm events were considered both drift-corrected and water balance

calibrated. The adjusted weir flowrates graphically validated. See **Figure 8** and **Figure 10** for the inflow and outflow rates of the pre and post water balance calibration.

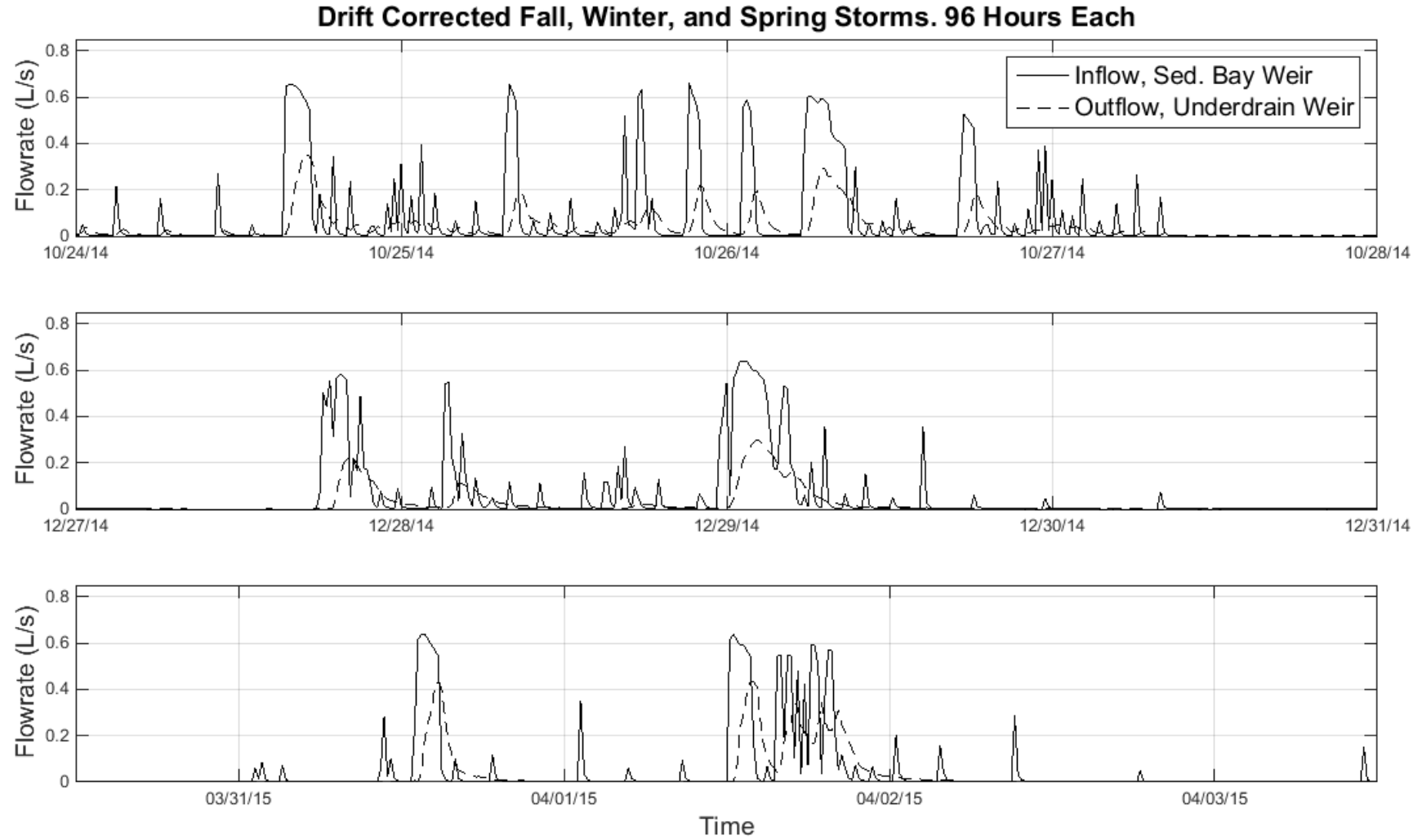


Figure 8. Drift corrected, pre-water balance calibrated flows. Storm events from fall 2014, winter 2014-2015, and spring 2015.

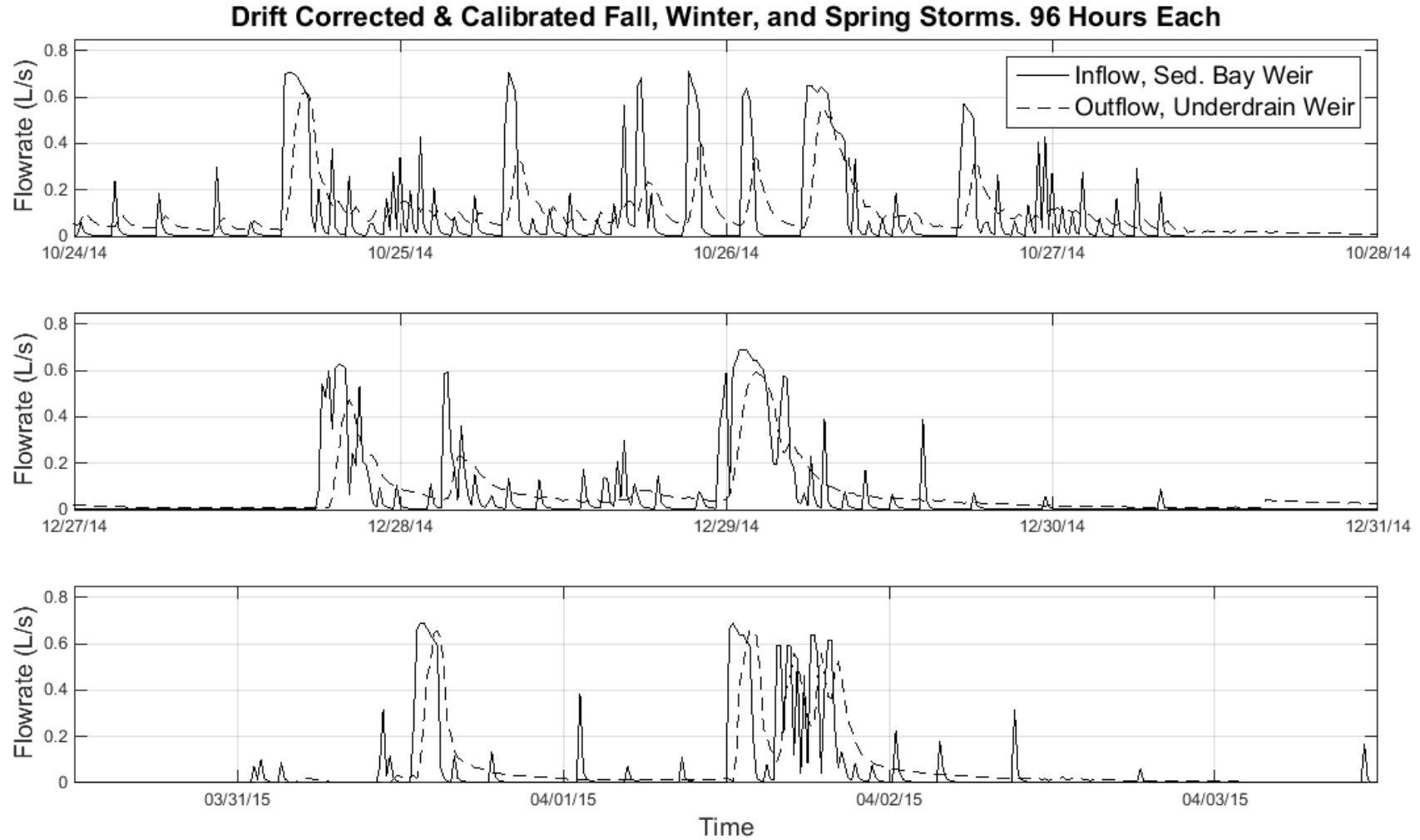


Figure 9. The drift corrected and water balance calibrated flow data were characteristic of the expected flow response: the water level drains to the bottom of the V before becoming relatively stable, and the outflow continues between peak flows due to gradual drainage of soil water.

The flowrate recession curve shapes followed the expected flow response in **Figure 9**. The water levels drains to the bottom of V-notch weir before stabilizing at a relatively constant value, and outflow continues between peak flows due to a gradual drainage of soil water, as expected. Therefore, the drift corrected and water balance calibrated underdrain flow data for the three storm events was graphically validated.

Peak Flow Response to Establishment Measured by Hydrologic Metrics

Peak flow ratio and the peak delay metrics (Eqn. 4 - 5) and their statistics were calculated for the fall, winter, and spring seasons. An attempt to apply the calibrated h_{weir} values from the three storm events to the remainder of the drift corrected data was made, however the volume balance showed a greater outflow volume than inflow volume, indicating that a need for additional water balance calibrations were required before the whole dataset could be rigorously validated. Therefore, the analyzed data set consisted of the water balance calibrated flow data from the three storm events along with the remainder of the drift corrected flow data that had not yet been water balance calibrated. Future work should include completion of the water balance calibration for the remainder of the dataset.

Matlab's built in "findpeaks.m" function was parameterized to find storm event peaks from the full dataset for statistical analysis using the three storm events as a way to calibrate the peak finder (**Figure 10**). The following parameters were used to identify outflow peaks: a minimum outflow peak height of 0.1 L/s, a minimum time lapse between peaks of 1 hour, and a minimum peak prominence of 0.05 L/s. Inflow peaks were paired with outflow peaks by finding local maxima near outflow peaks.

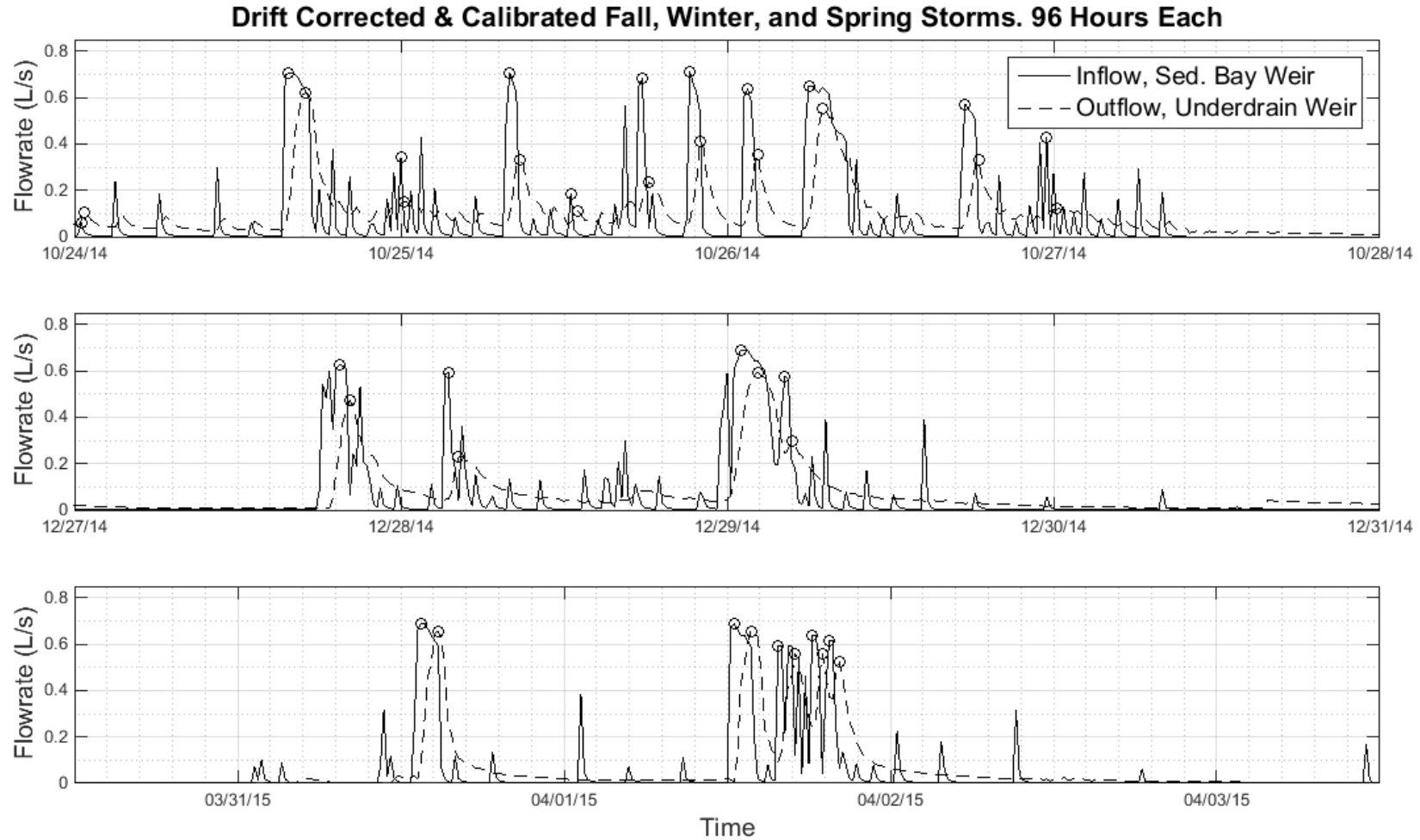


Figure 10. The peak finder was parameterized using the three storm events, and then it was used to find the peaks from the remainder of the drift corrected dataset.

The peak finder was then used to find peaks for the remainder of the dataset. A total of 64 peaks were paired for the fall, 23 for the winter, and 25 for the spring. A one-way ANOVA was used to test the statistical significance of the change in peak ratio and peak delay during the three seasons. The null hypothesis for this test is that the mean peak metrics of the different season are the same, and the alternative hypothesis is that at least one of the mean peak metrics are not the same. Histograms of the peak metrics, see **Figure 11** and **Figure 12**, were used to verify the assumption of equal variance and normal probability plots were used to verify normality for the one-way ANOVA. The distributions were considered to have similar spreads and be normally distributed, however, a larger data set and an improved peak finder would improve the validity of the Analysis of Variance (ANOVA) assumptions of equal variance, normality, and independence of observations.

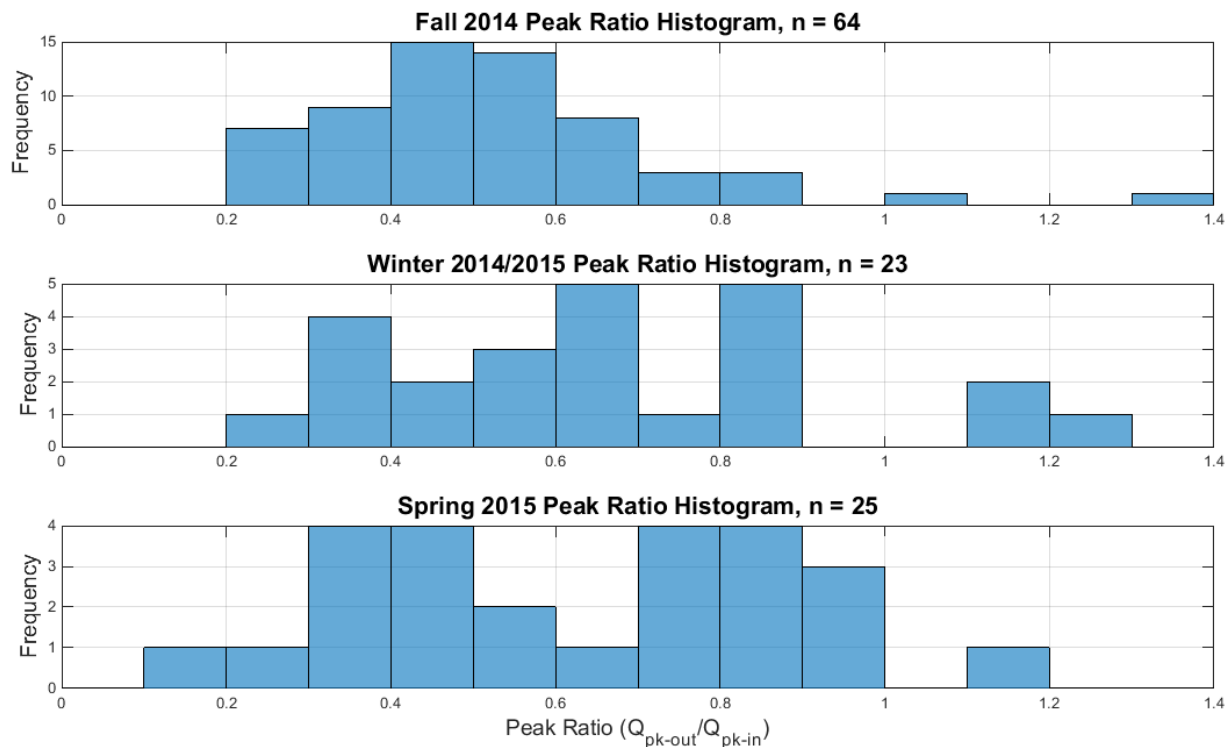


Figure 11. Histogram of peak ratio for each season. The distributions have a similar range of variance, which validates the assumption of similar spreads for the 1 way ANOVA.

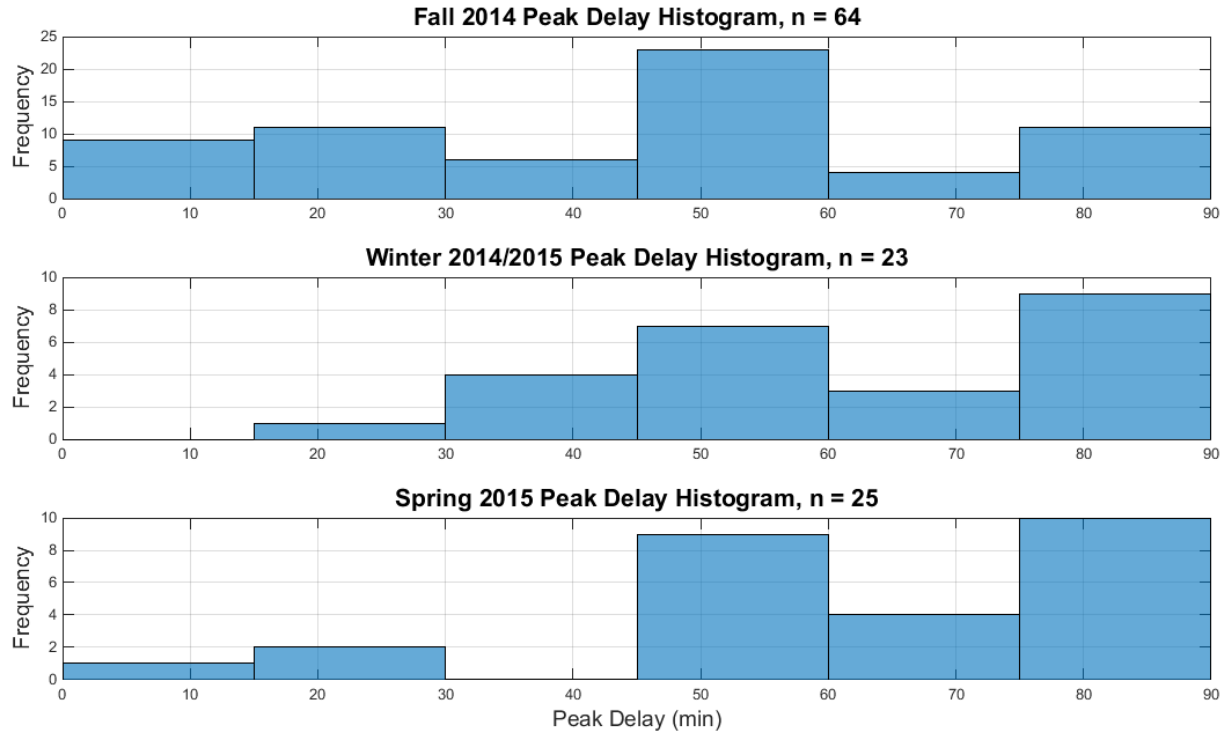


Figure 12. Histogram of peak delay for each season. The distributions have a similar range of variance, which validates the assumption of similar spreads for the 1 way ANOVA.

The mean peak ratio increased from 0.54 in the fall, to 0.68 in the winter, and then it decreased to 0.61 in the spring. The mean peak delay increased from 45 minutes in the fall, to 63 minutes in the winter, and then it decreased to 59 minutes in the spring. A general trend of an increase in response magnitude followed by decrease was observed. The p-values from the one way ANOVA for the peak ratio and peak delay are 0.090 and 0.0042, respectively, and a significance level of 5%, ($\alpha=0.05$), was used to test for statistical significance. There was no statistically significant evidence to reject the null hypothesis for the mean peak ratio statistical test, however, there is a moderate amount of evidence that at least one season has a significantly different mean peak delay than the other seasons ($p < 0.01$). See Table 5 for a summary of the peak ratio and peak delay statistics.

Peak Ratio (Q_{pk-out}/Q_{pk-in})			
Statistic	Fall 2014	Winter 2014-2015	Spring 2015
Mean	0.54	0.68	0.61
Median	0.51	0.63	0.61
Min	0.22	0.24	0.14
Max	1.69	1.25	0.95
Std. Dev.	0.25	0.27	0.25
Peak Ratio ANOVA			
F-Value	2.5		
P-Value	0.090		
Peak Delay (minutes)			
Statistic	Fall 2014	Winter 2014-2015	Spring 2015
Mean	45	63	59
Median	45	60	60
Min	0	30	0
Max	90	90	90
Std. Dev.	25	24	24
Peak Delay ANOVA			
F-Value	5.8		
P-Value	0.0042		
n	64	23	25

Table 5. Peak ratio and peak delay statistics. The low P-value for the one-way ANOVA test on differences between means for the peak delay was statistically significant.

Drain Tests

A drain test was performed on November 9-10 and March 23-24 to characterize the establishment's effect on outflow rate through the bioretention facility. The results from the tests were plotted on the same figure for comparison (**Figure 13**). The curves are characterized by a sharp peak followed by a gradual recession curve. The sharp peaks were produced immediately after the underdrain valve was opened. The majority of the head behind the weirs, $h_{measured}$, decrease in 15 minutes for Test #1, and decreased in 1 hour and 15 minute for Test #2. Test #2 is characterized by a more gradually slope recession curve than Test #1.

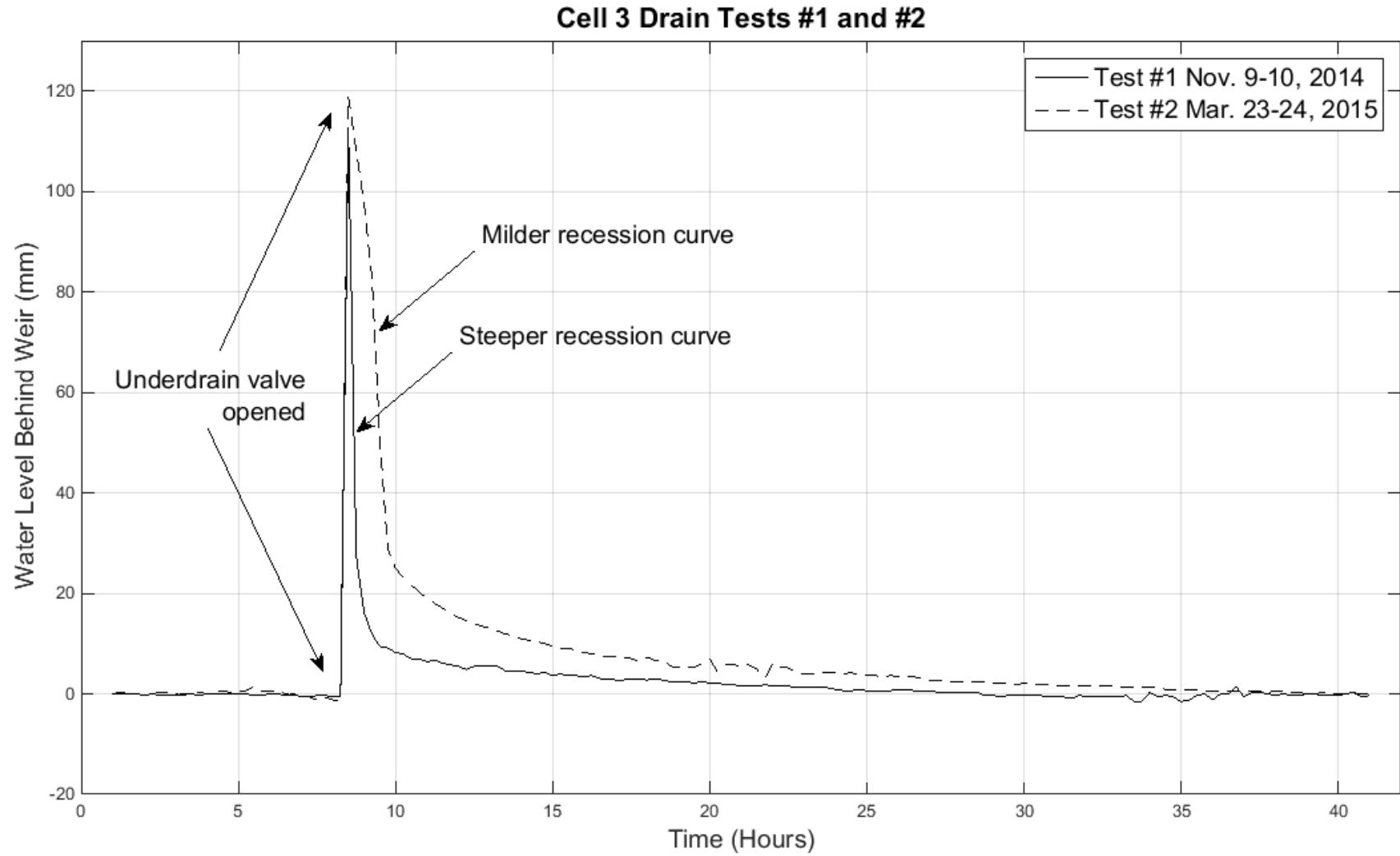


Figure 13. Results from the drain tests are characterized by sharp peaks followed by gradual recession curves. The recession curve in Test #2 had a more gradual slope than Test #1.

DISCUSSION

Pressure Transducer Drift Correction

The observed pressure transducer drift was detected by observations of the moving baseline for the water level at the bottom of the V-notch weirs following a storm event during which time $h_{\text{measured}} = h_{\text{weir}}$. Drift is common in fine level water measurement, and it tends to increase over time (Sorensen and Butcher 2011). The physical conditions exposed to the sediment bay pressure transducer were the following: after a storm event passed, the sediment bay water level decreased for approximately 2 hours until it reached the bottom of the V-notch weir. No additional flow into the bioretention cells was observed after approximately 2 hours. When the weather was warm and sunny, the water level in the sediment bay would continue to decrease after a storm at a rate slower than the first 2 hours due to evaporation. Therefore, storm events produced consistent patterns that were observed in the measured water level data, and this pattern could be used to apply a drift correction, similar to previous literature (LeFevre et al. 2009).

The baseline value for h_{weir} changed as frequently as from one storm event to the next, and possibly during the middle of a storm. When the value of h_{weir} changed, yet a similar storm pattern (due to the automatic pump) was observed, the pressure transducer drift was detected. Based on these patterns of the physical system, the value for h_{weir} was adjusted to account for the pressure transducer drift. However, the water balance was still not balanced after the drift correction, therefore further calibration of the value for h_{weir} was required, which led to the use of the water balance calibration procedure. Therefore, while the drift correction improves the expected pattern of the water level response, it does not account for all of the error associated with the inflow and outflow calculations, and further calibration can be accomplished with a water balance approach.

Water Balance Calibration

After the drift was corrected, the need for further calibration of the water level data was determined because the total cumulative outflow volume was only 59% of the total cumulative inflow volume. Greater confidence was given in the sediment bay water level data (inflow) than the underdrain water level data (outflow) because the inflow water level response had fewer uncertainties to affect the measured water depth. The sediment bay water level measurement response was primarily affected by pumped inflow, therefore a consistent pattern for the recession curve from the sediment bay was observed. Unlike the inflow, the underdrain outflow response was characterized by an inconsistent recession curve pattern due to gradual drainage of water from the soil that was affected by the establishment process (fines accumulation at the surface and soil compaction. Therefore, the sediment bay water level response pattern was more uniform in time than the underdrain outflow response pattern, and greater confidence could be given in the inflow pattern from which the outflow water level data could be calibrated.

The underdrain outflow water level was calibrated by adjustment of its height to account for the residual of the bioretention cell water balance for three 96 hour storm events during the fall, spring, and winter. After the calibration, the inflow and outflow data matched well with the expected response because their peaks and recession curves followed the expected flow model of a gradual decrease in water level to the bottom of the V-notch weirs. Nothing unusual, such as an outflow peak with a much greater magnitude than an inflow peak, or a recession curve that stabilized above zero, was detected in the calibrated dataset.

Bioretention Establishment

Peak Flow Analysis

The results of the peak flow metrics (**Table 5**) for each season were within the range of results reported by previous studies (**Table 1**). The mean peak ratio was 0.54 for the fall, 0.68 for the winter, and 0.61 for the spring, which falls into the literature value range of 0.01 to 0.86 (Table 1). The mean peak delay was 45 minutes for the fall, 63 minutes for the winter, and 59 minutes for the spring, which falls into the literature value range of 16 minutes to 309 minutes (Table 1). The large range for peak ratio and peak delay reported in the literature can be used to quantify the variability in hydrologic function from one stormwater facility to another. The calculated means for the peak ratio and peak delay from this study were similar to previous literature. However, the large range of values reported in the literature is an indication of the need for a greater understanding of effect of establishment on the hydrologic function of bioretention systems.

The p-values for the ANOVA on the peak ratio and peak delay metrics were 0.090 and 0.0042 (Table 5), respectively, indicating no significantly different peak ratio means, but at least one significant different mean peak delay. The inflow peak magnitude had a relatively consistent magnitude due to the automatic pump in the underground storage tank, and therefore the outflow peak magnitude could also be expected to have a relatively consistent magnitude. This explains the lack of significantly different peak ratio mean values throughout the monitoring period. The lower ANOVA p-value, and therefore greater confidence, of at least one season containing a different mean peak delay metric than the other seasons is explained using the bioretention conceptual model below

The trend of an increase in mean peak delay from the fall to the winter followed by a slight decrease in the spring was observed and found to be consistent with the bioretention establishment conceptual model (See Figure 1 and explanation below). Previous work investigating establishment has shown a decrease in soil permeability for 6 months (Summer 2006 – Winter 2006) followed by an increase for the remainder of the 18 month monitoring period at Monash University in Australia (Hatt et al. 2009). The initial decrease in permeability was attributed to soil compaction from hydraulic loading along with soil surface clogging due to stormwater sediment fines in the influent soil. The following increase in permeability was attributed to vigorous vegetation growth. In (Greene et al. 2009), they found that permeability was greatest in bioretention treatments with vegetation and earthworms compared to their control treatment of bare soil. This is explained by preferential flow path development causing an increase in soil permeability (Le Coustumer et al. 2012).

The trend of the initial increase in elapsed time for the peak delay was attributed to a decrease in soil permeability from soil compaction and fines accumulation. In this study, soil compaction was observed at the beginning of the establishment, especially during any activities that involved walking on the facility, and after storm events. During planting (Fall 2014) and weeding (Winter 2015) activities that involved digging into the soil, the compaction was observed to be greater at the surface than the subsurface. An accumulation of fine particles from the parking lot and road-construction-equipment yard on the surface of the bioretention cell was also observed. These observations are consistent with previous observations in the literature (Greene et al. 2009);(Hatt et al. 2009).

The soil compaction and fine particle accumulation explain the decrease in permeability observed between the two drain tests. The change in water level at the underdrain outflow weir was used to characterize the change in outflow rate during establishment. The drain test in March 2015, before substantial plant growth occurred, showed a milder sloped outflow recession curve compared to the November 2014 drain test (**Figure 13**). The milder sloped outflow recession curve was attributed to a lower rate of soil permeability. The moment that the soil surface becomes saturated is when ponding starts, and under soil conditions of low permeability, surface ponding occurs more readily (Dingman 2014). The soil surface becomes rapidly saturated due to soil compaction and clogging, which is followed by gradual ponding of stormwater influent. This allows for greater water storage at the surface from the inflow peak and increases the time until outflow peak arrival. Therefore, the observed trend of an increase in peak delay from 45 minutes in the fall to 63 minutes in the winter was attributed to a decrease of soil permeability caused by surface compaction and clogging.

Shortly after the second drain test in March 2015, the invasive weed species from the bioretention cell were removed by hand weeding, and the plants started growing vigorously (**Figure 14**). The plant growth observed during the spring corresponds with the trend of the decrease in the mean peak delay from 63 minutes to 59 minutes, however the mean winter peak delay was not significantly different from the spring peak delay (one-tailed t-test, $p = 0.22$). There were more storm events earlier in the spring than later in the spring, therefore the peak flow data is more representative of an earlier stage of establishment in the spring. The length of this study was only 7 months, compared to Hatt et. al 2009 which was 18 months, indicating that further increases in soil permeability, and thus decreases in peak delay, are hypothesized to occur with time. Future

drain tests and flow monitoring in the wet seasons of 2015 should be used to further validate the bioretention conceptual model after the summer growing months to determine if there is a greater response of the decrease of the peak delay.



Figure 14. Photos of plant growth throughout the monitoring period.

Error Analysis

Flowrate Calculations

The drift corrected and water balance calibrated water level datasets were sources of error for the peak flow metric analysis. The peak ratio was subject to greater error than the peak delay because the peak ratio depends on the magnitude of the peaks, while the peak delay only depends on the relative location of the peaks. The peak flow magnitudes, which were used for the peak ratio calculations (**Eqn. 4**), were subject to error from the water level measurements. The accuracy of each of the pressure transducers measured water depth are specified in the methods; a value of $\pm 3.8\text{mm}$ (the 1.5m range SDX) was used for the following analysis.

The error associated with the pressure transducer reporting a value lower than the true value is the under measured depth, and the error associated with the pressure transducer reporting a value higher than the true value is the over measured depth (**Figure 15**).

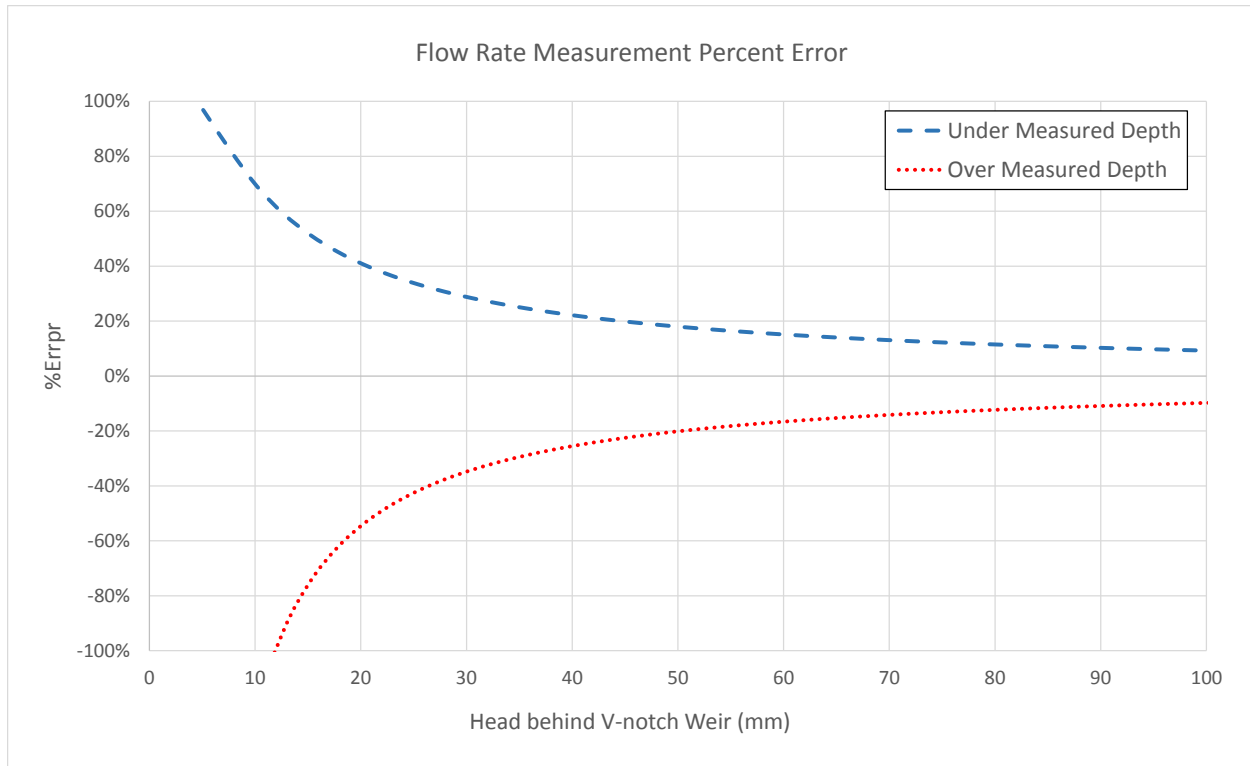


Figure 15. Variation of error with water depth for the inflow rate measurements. The error decreases exponentially as the head behind the V-notch weir increases.

The flow rate calculation error decreases exponentially as the value of head of water behind the weir, h_v , increases. The mean inflow peak magnitude was 0.59 L/s, which corresponds to an under measured depth error of 15% and an over measured depth error of 16% of the true value. The mean outflow peak magnitude was 0.43 L/s, which corresponds to an under measured depth error of 16% and an over measured depth error of 18% of the true value. The error associated with sediment bay water level measurements for the inflow calculations at the pump's full capacity of approximately 0.75 L/s per cell was 13% to 14% of the true value. An example of how the 1.5m range SDX pressure transducer accuracy of 3.8mm affects the flow rate measurements can be seen in **Figure 16**.

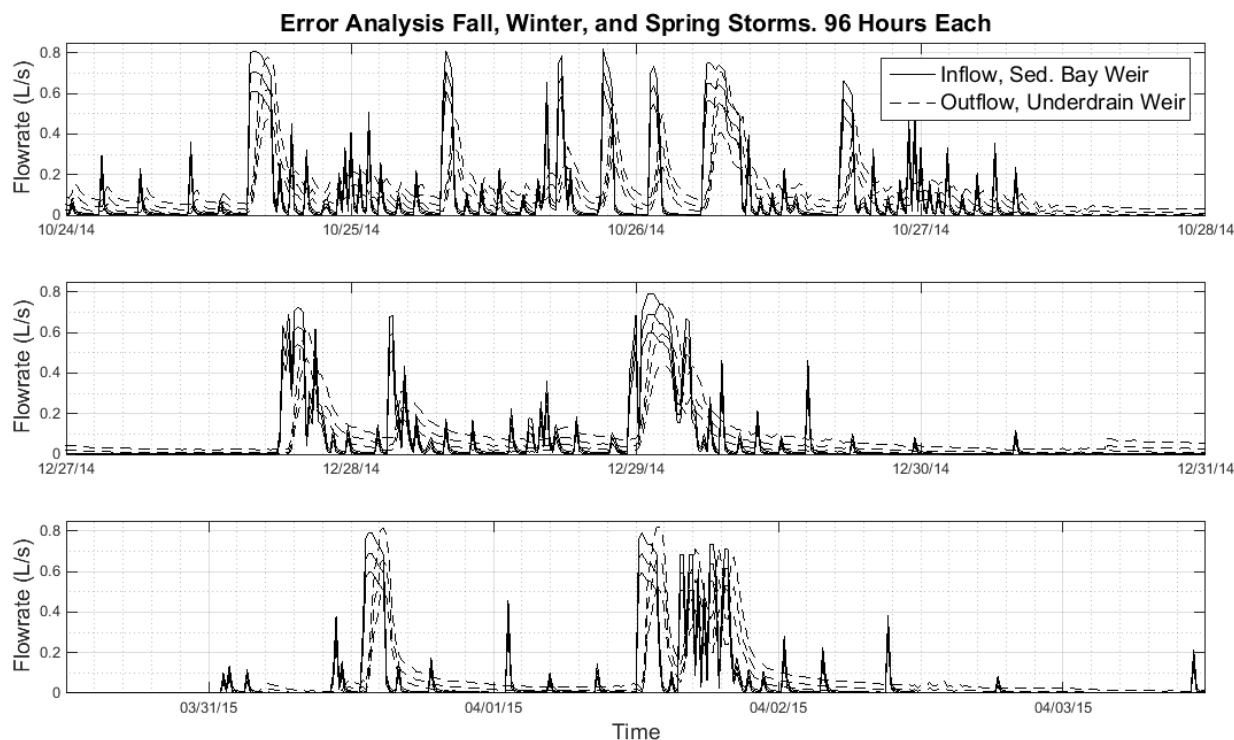


Figure 16. The range of error for the inflow and outflow measurements based on a 3.8mm accuracy of the 1.5m SDX pressure transducers. The three lines for the inflow and outflow rates are the minimum, mean, and maximum estimated flowrates based on the manufacturer's specified water level measurement error.

A greater magnitude of error occurs for the underdrain outflow measurement because the peaks were generally of lesser magnitude and the geometry of the compound weir, with a 2.5cm 90° V-notch and 7.6cm rectangular weir configuration, is such that a smaller change in water depth is associated with a greater change in flowrate measurement.

Additional Sources of Pressure Transducer Measurement and Flow Calculation Error

A study that investigated the error of 14 leading brand pressure transducers for fine water level measurement in the field found that the typical accuracy was reported as about ± 10 mm, and that measurement drift ranged from negligible to 27 mm for their 100 day monitoring period (Sorensen and Butcher 2011). Another study that investigated the correlation between measured sensor error and temperature in vented pressure transducers found that the noise in the measurement increased

as temperature increased under both laboratory and field conditions (Liu and Higgins 2015). While the three storms that used drift corrected and water balance calibrated data for flowrate calculation were graphically validated, a more rigorous study aimed at investigating sensor error would improve the confidence in these methods.

The drift correction error could be reduced by using physically measured values of h_{weir} with a staff gauge before and after every storm event, as mentioned in (Hatt et al. 2009) and (LeFevre et al. 2009). Additionally, investigation of the relationship between atmospheric pressure, vented tube length, and pressure transducer reading may allow for the development of additional methods to improve the drift correction. Finally, more accurate water level data could be measured with higher quality pressure transducers and with shorter time-steps (1 or 5 minute instead of 15 minutes) between measurements, or an increased scanning and reporting time.

The water balance includes multiple sources of data, including Hargreaves method with Samani correction for evapotranspiration estimates, precipitation data, and soil moisture data. Each one of these sources of data influences the water balance calibration. However, both the evapotranspiration and precipitation were an order of magnitude smaller than the inflow and outflow data, so the error associated with the use of these data for the water balance was considered negligible. However, the estimated volumetric change in soil moisture content was on the same order of magnitude as the inflow and outflow data for the fall, winter, and spring storm events. This source of error in the water balance calibration could be addressed with additional soil moisture sensors to improve the estimate for volumetric soil moisture content.

In this particular bioretention facility setup, a second water balance that uses the precipitation data along with water level data in the underground storage tank and a runoff and pump model could be used to further validate the calibration of h_{weir} for the sediment bay inflows. Greater confidence could then be put into the sediment bay inflow volume for the water balance calibration of the underdrain h_{weir} value for outflow calculations.

Another possible source of error is in the weir equation used for the inflow measurement and the rating curve used for the underdrain outflow measurement. V-notch weir thickness should be between 0.79mm (1/32 in.) and 1.6mm (1/16 in.) (Shen 1981). The inflow weir is made of 6.4 mm (1/4 in.) stainless steel, therefore the applicability of the v-notch weir equation for this thickness of weir is questionable. A flume experiment with the sediment bay v-notch inflow weirs could be used to develop a rating curve to check the accuracy of the standard V-notch weir equation. The discharge table developed by Thel-Mar was linearly interpolated to account for measured values not included in the discharge table, and the manufacture's specified flowrate accuracy was 5%. The methods the manufacturer used to determine this accuracy are unknown, therefore, the accuracy of the Thel-mar weir could also be verified with a flume experiment.

CONCLUSIONS

A bioretention cell was monitored for hydrologic function response to establishment between October 2014 and May 2015. The fine water level sensor measurements used for flowrate calculations were observed to drift by as much as 29mm over 93 days, and a graphically based drift correction method was applied to fix the drift. Further calibration of the flowrate calculations for three storm events was completed using a water balance approach. The results of the drift correction and water balance calibration were graphically validated to follow the expected pattern of a decrease in water level to the bottom of the v-notch, followed by a period of water level stabilization.

To the best of this author's knowledge, for the first time, peak flow metrics of peak ratio and peak delay were calculated for the fall, winter, and spring of the monitoring period to evaluate the peak hydrologic response of bioretention establishment on a seasonal basis. The mean peak ratio was 0.54 in the fall, 0.68 in the winter, and 0.61 in the spring. The mean peak delay was 45 minutes in the fall, 63 minutes in the winter, and 59 minutes in the spring. A one-way ANOVA p-value of 0.090 for the peak ratio indicated that the differences in peak ratio observed between the seasons were not significant. However, a p-value of 0.0042 for the peak delay, along with a t-test comparing the mean delays of the winter and spring storm events, indicated that at least one of the seasons (the fall) has a peak delay value that is significantly different from the other seasons. The trend of an increase in peak delay from fall to winter was attributed to changes in soil permeability caused by soil compaction and clogging. This trend was further supported by an observed decrease in permeability observed during a drain test in November and March. A weak trend of a decrease in peak delay from winter to spring was attributed to preferential flow

path development caused by plant root growth. The peak ratio and peak delay metrics should be considered with caution due to the minimal validation of the drift correction and water balance calibration methods. Future work should attempt to minimize error in water level measurements for flow rate calculations, validate the drift correction and water balance calibration techniques, and use a longer term dataset to determine if there is a stronger response in the peak delay during the next wet season after the plants and soil continue to mature throughout the summer.

Considerations for Future Research in Bioretention

The indefinite period of bioretention establishment time poses more questions than answers. There are two competing changes to the soil permeability. On one hand, the permeability may decrease as soil compaction and clogging are likely to continue to occur, although the compaction may stabilize, while the surface clogging increases due to a continuous influx of fines from urban stormwater runoff. On the other hand, the permeability may increase as the plants continue to grow their roots and earthworms and soil organisms continue to develop macropores and preferential flow paths, but this rate of development may approach zero as the soil reaches its carrying capacity. Therefore, in the long run, permeability could decrease, as the fines continue to accumulate, but the other factors effecting permeability could stabilize, leading to an overall decrease in permeability. Long term research investigating how flows are affected by bioretention establishment will help to inform bioretention facility managers as to the type and schedule of maintenance activities required for meeting hydrologic objectives. Such activities may include replacement of the top several cm of soil media, introduction of macro-pore developing organisms, or re-vegetation efforts to maintain desired permeability.

Bioretention establishment hydrology is important to consider in design as these systems continue to be improved to meet hydrologic function objectives for both flood control and restoration of pre-development hydrologic regimes. The results of this work emphasize the importance of water level measurement validation when using weirs and pressure transducers for flow rate calculations, which is common in the bioretention literature. The results of this study suggest that peak flows are affected by bioretention establishment, but further research is needed to quantify the extent of the effect of establishment on hydrologic function.

BIBLIOGRAPHY

- Allen, R. G., Pereira, L. S., Raes, D., and Smith, M. (1998). "FAO Irrigation and drainage paper No. 56." *Rome: Food and Agriculture Organization of the United Nations*, 26-40.
- Barrett, M., Limouzin, M., and Lawler, D. (2012). "Effects of Media and Plant Selection on Biofiltration Performance." *Journal of Environmental Engineering*, 139(4), 462-470.
- Benner, P. (2015). "Communication regarding the historical ecosystems present at the project site."
- Brown, R., and Hunt, W. (2010). "Impacts of Media Depth on Effluent Water Quality and Hydrologic Performance of Undersized Bioretention Cells." *Journal of Irrigation and Drainage Engineering*, 137(3), 132-143.
- Brown, R. A., Skaggs, R. W., and Hunt Iii, W. F. (2013). "Calibration and validation of DRAINMOD to model bioretention hydrology." 486(0), 430-442.
- Carpenter, D., and Hallam, L. (2009). "Influence of Planting Soil Mix Characteristics on Bioretention Cell Design and Performance." *Journal of Hydrologic Engineering*, 15(6), 404-416.
- Clayden, A., and Dunnett, N. (2007). *Rain Gardens: Managing Water Sustainably in the Garden and Designed Landscape*, Timber Press, Inc.
- Cramer, K. (2012). "Reducing Combined Sewer Overflows to Puget Sound Using Green Stormwater Infrastructure." D. o. N. R. a. Parks, ed. King County, Washington.
- Davis, A. P. (2008). "Field performance of bioretention: Hydrology impacts." *Journal of Hydrologic Engineering*, 13(2), 90-95.
- Dingman, S. L. (2014). *Physical Hydrology*, Waveland Press, Inc.
- Emanuel, R., Godwin, D., and Stoughton, C. (2009). "The Oregon Rain Garden Guide."
- Emerson, C., and Traver, R. (2008). "Multiyear and Seasonal Variation of Infiltration from Storm-Water Best Management Practices." *Journal of Irrigation and Drainage Engineering*, 134(5), 598-605.
- EPA (1999). "Storm Water Technology Fact Sheet: Bioretention." O. o. Water, ed. Washington, D.C. .
- EPA (2013). "Case Studies Analyzing the Economic Benefits of Low Impact Development and Green Infrastructure Programs." O. a. W. Office of Wetlands, ed. Washington, D.C.
- EPA, U. S. (1993). "Natural Wetlands and Urban Stormwater: Potential Impacts and Management.", O. a. W. W. D. Office of Wetlands, ed. Washington, D.C.
- Extension, O. (2014). "LID Infiltration Facility Calculator."
- Fletcher, T. D., Andrieu, H., and Hamel, P. (2013). "Understanding, management and modelling of urban hydrology and its consequences for receiving waters: A state of the art." *Advances in Water Resources*, 51(0), 261-279.
- Garrison, N., Hobbs, K., Beckman, D., Devine, J., Berzins, A., Clifton, E., Levine, L., and Hammer, R. (2013). "Rooftops to River II: Green strategies for controlling stormwater and combined sewer overflows." Natural Resources Defense Council (NRDC).
- Greene, A., Hutchinson, S., Christianson, R., and Moore, T. (2009). "Impacts of Biota on Bioretention Cell Performance during Establishment in the Midwest." *World*

- Environmental and Water Resources Congress 2009*, American Society of Civil Engineers, 1-13.
- Hans, K. (2015). "Communication regarding the fish species identified in the Mill Race channel."
- Hatt, B. E., Fletcher, T. D., and Deletic, A. (2009). "Hydrologic and pollutant removal performance of stormwater biofiltration systems at the field scale." *Journal of Hydrology*, 365(3-4), 310-321.
- Hollis, G. E. (1975). "The effect of urbanization on floods of different recurrence interval." 11(3), 431-435.
- Hsieh, C. H., and Davis, A. P. (2005). "Evaluation and optimization of bioretention media for treatment of urban storm water runoff." *Journal of Environmental Engineering-Asce*, 131(11), 1521-1531.
- Hunt, W. F., SMith, J. T., Jadlocki, S. J., Hathaway, J. M., and Eubanks, P. R. (2008). "Pollutant Removal and Peak Flow Mitigation by a Bioretention Cell in Urban Charlotte, N.C." *Journal of Environmental Engineering*, 134(5), 403-408.
- Le Coustumer, S., Fletcher, T. D., Deletic, A., Barraud, S., and Poelsma, P. (2012). "The influence of design parameters on clogging of stormwater biofilters: A large-scale column study." *Water Research*, 46(20), 6743-6752.
- LeFevre, N., Watkins, D., Gierke, J., and Brophy-Price, J. (2009). "Hydrologic Performance Monitoring of an Underdrained Low-Impact Development Storm-Water Management System." *Journal of Irrigation and Drainage Engineering*, 136(5), 333-339.
- Leopold, L. B. (1975). *Hydrology for Urban Land Planning - A Guidebook on the Hydrologic Effects of Urban land Use*, United States Geological Survey.
- Liu, J., Sample, D., Bell, C., and Guan, Y. (2014). "Review and Research Needs of Bioretention Used for the Treatment of Urban Stormwater." *Water*, 6(4), 1069-1099.
- Liu, Z., and Higgins, C. W. (2015). "Does temperature affect the accuracy of vented pressure transducer in fine-scale water level measurement?", 4(1), 65-73.
- Low Impact Center Development, I. (2015). "LID Urban Design Tools."
- Meierdiercks, K. L., Smith, J. A., Baeck, M. L. and Miller, A. J. (2010). "Analyses of Urban Drainage Network Structure and its Impact on Hydrologic Response."
- Muthanna, T. M., Viklander, M., and Thorolfsson, S. T. (2008). "Seasonal climatic effects on the hydrology of a rain garden." *Hydrological Processes*, 22(11), 1640-1649.
- Paus, K., Morgan, J., Gulliver, J., and Hozalski, R. (2014). "Effects of Bioretention Media Compost Volume Fraction on Toxic Metals Removal, Hydraulic Conductivity, and Phosphorous Release." *Journal of Environmental Engineering*, 140(10), 04014033.
- Poresky, A., and Palhegyi, G. (2008). "Design and Modeling of Bioretention for Hydromodification Control: An Assessment of Alternative Model Representations." *Low Impact Development for Urban Ecosystem and Habitat Protection*, American Society of Civil Engineers, 1-10.
- Roy-Poirier, A., Champagne, P., and Fillion, Y. (2010). "Review of Bioretention System Research and Design: Past, Present, and Future." *Journal of Environmental Engineering*, 136(9), 878-889.
- Samani, Z. (2000). "Estimating solar radiation and evapotranspiration using minimum climatological data." *Journal of Irrigation and Drainage Engineering*.
- Shen, J. (1981). "Discharge Characteristics of Triangular-notch Thin-plate Weirs." D. o. t. Interior, ed., United States Government Printing Office, Washington, 62.

- Sorensen, J. P. R., and Butcher, A. S. (2011). "Water Level Monitoring Pressure Transducers—A Need for Industry-Wide Standards." *Ground Water Monitoring & Remediation*, 31(4), 56-62.
- Walsh, C. J., Roy, A. H., Feminella, J. W., Cottingham, P. D., Groffman, P. M., and Morgan, R. P. (2005). "The urban stream syndrome: current knowledge and the search for a cure." *Journal of the North American Benthological Society*, 24(3), 706-723.

APPENDIX A: PLANT LIST

	Plant Species	Intentially Added?
1	<i>Achillea millefolium</i>	x
2	<i>Camassia quamash</i>	x
3	<i>Carex densa</i>	x
4	<i>Carex obnupta</i>	x
5	<i>Danthonia californica</i>	x
6	<i>Deschampsia cespitosa</i>	x
7	<i>Eschscholzia</i>	
8	<i>Fragaria virginica</i>	x
9	<i>Gaultheria shallon</i>	x
10	<i>Juncus patens</i>	x
11	<i>Lupinus polyphyllus</i>	x
12	<i>Mahonia repens</i>	x
13	<i>Matricicaria discoidea</i>	
14	<i>Mimulus guttatus</i>	x
15	<i>Potentilla gracilis</i>	x
16	<i>Rosa nutkana</i>	x
17	<i>Saxifraga oregana</i>	x
18	<i>Scirpus acutus</i>	x
19	<i>Sidalcea campestris</i>	x
20	<i>Symphoricarpos albus</i>	x